

Subaru/HDS study of CH stars: elemental abundances for stellar neutron-capture process studies^{*}

Aruna Goswami¹, Wako Aoki², Drisya Karinkuzhi¹

¹Indian Institute of Astrophysics, Koramangala, Bangalore 560034, India; aruna@iiap.res.in; drisya@iiap.res.in

²National Astronomical Observatory, Mitaka, Tokyo, 181-8588 Japan; aoki.wako@nao.ac.jp

Accepted : Received : in original form :

ABSTRACT

A comprehensive abundance analysis providing rare insight into the chemical history of lead stars is still lacking. We present results from high resolution ($R \sim 50\,000$), spectral analyses of three CH stars, HD 26, HD 198269, HD 224959, and, a carbon star with a dusty envelope, HD 100764. Previous studies on these objects are limited by both resolution and wavelength regions and the results differ significantly from each other. We have undertaken to re-analyse the chemical composition of these objects based on high resolution Subaru spectra covering the wavelength regions 4020 to 6775 Å. Considering local thermodynamic equilibrium and using model atmospheres, we have derived the stellar parameters, the effective temperatures T_{eff} , surface gravities $\log g$, and metallicities $[\text{Fe}/\text{H}]$ for these objects. The derived parameters for HD 26, HD 100764, HD 198269 and HD 224959 are (5000, 1.6, -1.13), (4750, 2.0 -0.86), (4500, 1.5, -2.06) and (5050, 2.1, -2.44) respectively. The stars are found to exhibit large enhancements of heavy elements relative to iron in conformity to previous studies. Large enhancement of Pb with respect to iron is also confirmed. Updates on the elemental abundances for several s-process elements (Y, Zr, La, Ce, Nd, Sm, Pb) along with the first-time estimates of abundances for a number of other heavy elements (Sr, Ba, Pr, Eu, Er, W) are reported. Our analysis suggests that neutron-capture elements in HD 26 primarily originate in s-process while the major contributions to the abundances of neutron-capture elements in the more metal-poor objects HD 224959 and HD 198269 are from r-process, possibly formed from materials that are pre-enriched with products of r-process.

Key words: stars: individual (HD 26, HD 198269, HD 224959, HD 100764) - stars: carbon- stars: CH- stars: CEMP-r/s- stars: Abundances- stars: Nucleosynthesis

1 INTRODUCTION

Slow neutron-capture (s-process) elements are mainly produced by thermally pulsating asymptotic giant branch (AGB) stars; however, there remains large uncertainties associated with the formation of the main neutron source ^{13}C . Observations of stars that show enhancement of s-process elements abundance can provide important constraints on theoretical models. CH stars (Keenan 1942) form good candidates to investigate the properties of s-process at low-metallicities as their spectra exhibit weak lines of the iron-group elements but enhanced lines of heavy elements. The stellar population of the Galactic halo is characterized by metal-poor low-mass stars, in which, Carbon-Enhanced Metal-Poor (CEMP) stars form a substantial fraction of the

objects with metallicity, $[\text{Fe}/\text{H}] \leq -2$. About 80% of the CEMP stars are known to be enriched with s-process elements (Lucatello et al. 2003, Aoki et al. 2007, Roederer et al. 2008). These objects are more metal-poor counterparts of CH stars. The chemical composition of these stars offer insights into the nucleosynthesis of heavy-elements. Chemical composition studies of CEMP stars (Barbuy et al. 2005, Norris et al. 1997a, b, 2002; Aoki et al. 2001, 2002a, b; Goswami et al. 2006, Goswami & Aoki 2010, Karinkuzhi & Goswami 2014, 2015) have suggested that a variety of production mechanisms are needed to explain the observed range of elemental abundance patterns in them; however, the binary scenario of CH star formation is currently considered as the most likely formation mechanism also for CEMP-s stars. Lucatello et al. (2005b) have demonstrated that all CEMP-s stars are likely members of binary systems. However, recent models of binary population synthesis are unable to reproduce the observed fraction of CEMP stars without invoking

^{*} Based on data collected at the Subaru Telescope, which is operated by the National Astronomical Observatory of Japan

non-standard nucleosynthesis or a substantial change in IMF (Abate et al. 2013). There exist different scenarios of carbon and s-process element production at low and near-solar metallicity stars. For the origin of the s-process isotopes with mass number $A \leq 90$, the activation of the $^{22}\text{Ne}(\alpha, n)^{25}\text{Mg}$ reaction appears the main production mechanism (Prantzos et al. 1987). This is referred as weak-s-process mechanism. For the production of the s-process nuclei with $A \geq 90$ (main component), the operation of the $^{13}\text{C}(\alpha, n)^{16}\text{O}$ in low-mass stars of rather low-metallicity seems to be a good site (Hollowell and Iben 1988). Neutron-capture process characterized by high flux of neutrons (r-process) is hypothesized by Truran (1981) to be responsible for the production of most neutron-capture elements at the early ages of the Galactic life. For the enhanced abundance of Eu with [Eu/Ba] ratios considerably higher than that resulting from s-process nucleosynthesis calculations, (these stars are classified as CEMP-r/s stars, Beers & Christlieb 2005), no convincing explanation is yet available. Except for the overabundance of Eu, the CEMP-r/s stars do not show any systematic difference from the CEMP-s stars. Although considerable theoretical and observational interest has been focussed on these stars much remains mysterious about them (i.e., Zijlstra (2004)). Our understanding of the range of physical phenomena involved in the formation processes of these objects still remains incomplete and needs to be substantiated by further observational and theoretical studies. In this work, we have undertaken to conduct fresh analysis of chemical compositions for stars HD 26, 198269 and 224959 listed in CH star catalogue of Bartkevicius (1996) and HD 100764, a carbon star known to have a dusty envelope. Previous studies on these objects are limited by both resolution and spectral coverage and differ significantly from each other. The fact that the results reported by Van Eck et al. (2003) for heavy elements such as Zr, La, Ce and Nd in three of the four CH stars which are based on better spectra are very different from those reported by Vanture (1992c) motivated us to re-estimate the chemical abundances, examine the extent to which our results confirm or contrast the previous results and hence understand their chemical history. It is towards this end that we have undertaken to conduct this study based on high resolution spectra obtained using HDS attached to 8-m Subaru telescope and re-evaluate the atmospheric parameters and the chemical compositions. The presence of several s-process elements such as Sr, Y, Zr, Ba, La, Ce, Nd, Sm are clearly evident from these spectra. We report new results on the chemical composition and discuss mechanisms giving rise to the overabundance of s-process elements in light of existing theories.

Models of very low-metallicity AGB stars developed in the frame work of the partial mixing of protons into the deep carbon rich layers, predict overabundances of Pb-Bi as compared to lighter s elements (Goriely & Mowlavi 2000). These stars, are characterized by large [Pb/Fe], [s/Fe] and [Pb/s] abundance ratios, where s represents s-process elements. In this scenario, AGB stars with $[\text{Fe}/\text{H}] \leq -1.3$, are predicted to exhibit [Pb/hs] (where hs, refers to heavy s-process elements, such as Ba, La, Ce) ratios as large as 1.5. These predictions are found to be quite robust with respect to the model parameters, i.e., the abundance profile of the protons in the partially mixed layers or the extent of the partial mixing zone and uncertainties in reaction rates. Low-

metallicity AGB stars that exhibit large overabundances of Pb-Bi compared to lighter s-elements are called as ‘lead-stars’. Although, HD 26, HD 198269 and HD 224959 are known as ‘lead-stars’, the abundance of the second-peak s-process element Ba, as well as other heavy elements such as Sr, Pr, Eu and Er etc. are not available in literature for these objects. We have determined the abundances of these elements from analyses of their high-resolution Subaru spectra. Radial velocity survey of McClure (1984), McClure and Woodsworth (1990), have confirmed binarity for three of these objects. As the chemical compositions of these stars can provide observational constraints for testing and building models of AGB nucleosynthesis, accurate determination of the stellar parameters and their chemical compositions is extremely important. Further, as these objects occupy a wide range in metallicity, the question of metallicity dependence of s-process can also be investigated considering a large sample of these objects and covering a wide range in metallicity.

Recent studies have indicated that classical CH stars and CEMP-s stars, probably belong to the same category (Masseron et al. 2010). If so, the population of these objects with accurate chemical history would be vital for understanding the contribution of low and intermediate mass stars to the chemical evolution of the Galaxy and other stellar systems.

In the next section we give a brief summary of the previous studies on these objects from literature and highlight the novel aspects of the present study. In section 3, we present details of observations, data analysis and estimates of radial velocities. In section 4, we present *BVRJHK* photometry of these stars, and give estimates of effective temperatures based on photometry. The methodology followed for deriving the stellar atmospheric parameters is discussed in section 5. The elemental abundance results are presented in section 6. Parametric model based analysis of the observed abundances is discussed in section 7. Discussion and concluding remarks are drawn in section 8.

2 PREVIOUS STUDIES - A SUMMARY

Some aspects of these objects were addressed by different authors in previous studies; here we summarize their main results.

Lee (1974): Lee carried out a detailed study on the chemical composition of HD 198269 based on three spectrograms having dispersion of 6.5 \AA mm^{-1} , 10 \AA mm^{-1} , and 178 \AA mm^{-1} respectively, obtained using KPNO 16 inch telescope. As the available data was not sufficient to warrant a detailed model atmosphere approach, a standard curve-of-growth analysis was performed. The analysis was done with respect to ϵ Vir, correcting line strengths for the difference in the effective temperatures of ϵ Vir and HD 198269. A metallicity ([Fe/H]) of -1.56 was adopted for this object. At this metallicity [C/Fe] was estimated to be $+1.92$.

Vanture (1992a, 1992b, 1992c): In a series of three papers Vanture had discussed carbon isotopic ratios, abundances of C, N, O and heavy elements (also Cu and Mo for HD 26) derived from an LTE analysis of the equivalent widths of weak atomic lines using modified version of MOOG (Snedden 1973). The analyses were based on spectra observed

with the 1.5-m telescope at the Cerro Tololo Inter American Observatory using the Fibre Fed Echelle with GEC CCD detector having resolutions of 0.24 Å in the blue and 0.44 Å in the red ($\lambda/\delta\lambda \sim 20,000$) with a S/N $\sim 80 - 150$ in both red and blue. Additional spectra for HD 26 and HD 224959 were obtained from 4-m telescope at Kitt Peak Observatory with resolution of 0.25 Å at 8000 Å ($\lambda/\delta\lambda \sim 32,000$) and S/N in the range 100 - 180.

Carbon isotopic ratios ($^{12}\text{C}/^{13}\text{C}$) were determined from spectrum synthesis calculations using the 1-0 C₂ Swan system at 4737 Å and the CN red system 2-0 band near 8000 Å. The derived values are > 25 for HD 26 (from both C₂ and CN) which is about a factor of 2 higher than that of Aoki & Tsuji (1997). For HD 198269, these estimates are respectively 4 and 6 and for HD 224959, 3 and 13.

Vanture used the Oxygen triplet lines of 7771, 7774 and 7775 Å to determine the abundances of Oxygen. These lines returned abundances that differed by 0.3 dex to 0.6 dex. Weak undetected lines blending with the oxygen lines was cited as the primary reason causing this difference. Spectrum synthesis method was also used around 6300 Å region to constrain the oxygen abundance in HD 198269 and HD 224959. As the spectrum of HD 26 around [O I] 6300 Å was not of high quality to set an upper limit for oxygen, the oxygen abundance for this star was adopted from near IR oxygen triplet lines alone.

Using oxygen abundance derived from O I triplet lines, carbon abundance in HD 26 was derived from spectral synthesis calculation of C₂ molecular band at 4737 Å. For the other two stars carbon abundances were determined from analyses of equivalent widths of the CH A²Δ - X²ΠΔν = -11 lines at 4835 and 4880 Å. Carbon abundance derived from CH lines were further checked by synthesizing the C₂(1,0) band at 4737 Å. Nitrogen abundance was determined from spectral synthesis of the CN Red system in the regions 7995 - 8013 Å and 8029 - 8042 Å. Final N abundance adopted is the average of the two values derived from these two spectral regions.

C, N, O abundances (log ε) for HD 26, derived with adopted metallicity ([Fe/H]) of -0.44 are respectively 8.4, 7.9 and 8.45. These abundances are 8.5, 8.2 and < 7.7 for HD 224959 and 7.9, 7.6 and < 7.6 respectively for HD 198269; the adopted [Fe/H] for HD 224959 and HD 198269 were respectively -1.6 and -1.4. We note that, Vanture's adopted metallicities vary significantly from our estimates of -1.13, -2.04 and -2.42 respectively for HD 26, HD 198269 and HD 224959.

Aoki & Tsuji (1997): These authors have derived carbon isotopic ratios ($^{12}\text{C}/^{13}\text{C}$) from spectral analysis of CN red system for HD 224959, HD 198269, and HD 100764. The values are respectively 7, 7 and 4. This ratio estimated using C₂ Swan system is ~ 10 for HD 26. These values are estimated at effective temperatures that compare closely to our estimates. However, metallicities differ significantly. Low values (< 10) of ($^{12}\text{C}/^{13}\text{C}$) qualify the objects to be early type CH stars that are post-mass-transfer binary systems (McClure & Woodsworth 1990). In Table 1, we have summarized the literature values of C, N, O abundances with respect to Fe as well as $^{12}\text{C}/^{13}\text{C}$ ratios.

Van Eck et al. (2001, 2003): The first detection of lead in HD 26, HD 198269 and HD 224959 were reported in these papers. Abundances for C, heavy elements Zr, La, Ce,

Nd and Sm were also presented. The results are based on two separate observations; i) medium resolution spectra of two spectral windows containing Pb lines obtained at Observatoire de Haute Provence (OHP) in Aug 2000; ii) high-resolution spectra obtained at ESO in Sep 2000. The OHP spectra were obtained with 1.52m telescope at a resolution of $\lambda/\delta\lambda \sim 85,000$ in the 2nd order at 720 nm to explore the 722.897 nm Pb I line and 3000 rule mm^{-1} holographic grating was used to explore the 401.963, 405.781 and 406.214 nm Pb I lines with a resolution of 45000. The ESO spectra were obtained on the Coude Echelle Spectrometer (CES) fed by the 3.6-m telescope. A resolution of 135,000 was achieved at the central wavelength of 405.8 nm. The spectra covered a wavelength range of 404.5 - 407.1 nm.

The s-scatter rather than the r-process was believed to be responsible for the observed overabundances of heavy elements. The authors concluded that HD 224959 and HD 198269 belong to the class of 'lead stars', since their [Pb/Fe] ratios comply with the prediction for the standard model for Partial Mixing of Protons (PMP) operating in low-metallicity AGB stars.

Novel aspects of the present work: The present results are based on a detailed abundance analysis based on high-resolution ($R \sim 50,000$) spectra obtained with Subaru using HDS (Noguchi et al. 2002). The wavelength coverage is continuous from 4020 through 6775 Å except for a small gap of about 75 Å from 5335 Å to 5410 Å. Van Eck et al. used a higher resolution spectra for obtaining Pb abundances but the wavelength coverage is limited to 4045 - 4071 Å. In determining the stellar atmospheric parameters (T_{eff} , log g, and [Fe/H]), from an LTE analysis of the equivalent widths of atomic lines of Fe, we have used the most recent version of the spectrum synthesis code MOOG (Snedden 1973) with standard assumptions of Local Thermodynamic Equilibrium, plane parallel atmosphere, hydrostatic equilibrium and flux conservation. We have made use of the new grid of ATLAS09 model atmospheres of Kurucz database (<http://kurucz.harvard.edu/grids.html>). Our analysis is also benefited by the fact that we have used an extensive line-list for heavy elements (Table 13) in consultation with the most updated and well tested log gf values. We have measured the equivalent widths for a large number of lines in the solar spectra, that are common in our program stars spectra and measured the solar abundances using the log gf values that we have adopted. The solar atmospheric parameters used are $T_{eff} = 5835$ K, $\log g = 4.55$ cm s^{-2} and micro turbulent velocity 1.25 km s^{-1} . The derived abundances match closely within a range of 0.08 - 0.1 dex, when comparing with Asplund (2009). We have presented the first-time estimates of abundances for the heavy elements Sr, Ba, Pr, Eu, Er and W. We have also performed a parametric model based analysis of the observed abundances to examine the relative contributions from the s- and r-process to the observed abundances of heavy elements in order to understand the underlying nucleosynthesis responsible for the observed abundances.

Table 1: CNO abundances from the literature

Star	$^{12}\text{C}/^{13}\text{C}$ (4737 Å)	$^{12}\text{C}/^{13}\text{C}$ (8000 Å)	[C/Fe]	[N/Fe]	[O/Fe] (6300 Å)	[O/Fe] (7777 Å)	Ref
HD 26	-	-	0.31	1.12	0.34	-	1
	≥ 25	≥ 25	0.41	0.51	-	0.20	2
	-	9	0.68	0.94	0.36	-	3
HD 198269	-	-	2.31	1.77	0.33	-	1
	-	-	1.92	-	-	-	4
	4	6	0.87	0.91	-	0.05	2
HD 224959	-	-	2.01	1.98	0.34	-	1
	3	13	1.67	1.97	-	0.61	2
	-	4	1.77	1.88	1.10	-	3

1. This work, 2. Vanture (1992a), 3. Masseron et al. (2010), 4. Lee (1974)

3 OBSERVATION, DATA REDUCTION, AND RADIAL VELOCITIES

High-resolution spectra for the objects were obtained using the High Dispersion Spectrograph (HDS) attached to the 8.2m Subaru Telescope (Noguchi et al. 2002) on May 30, 2004 (HD 224959) and June 1, 2004 (HD 26, HD 100764 and HD 198269). Each object spectrum was taken with a 5 minutes exposure having a resolving power of $R \sim 50\,000$. The observed bandpass ran from about 4020 Å to 6775 Å, with a gap of about 75 Å, from 5335 Å to 5410 Å, due to the physical spacing of the CCD detectors. The data reduction was carried out, in the standard fashion, using IRAF¹ spectroscopic reduction package. The basic parameters of these objects are listed in Table 2.

3.1 Radial velocities

The radial velocities of our program stars are measured using several unblended lines. Estimated heliocentric radial velocities v_r of the program stars are presented in Table 3. Previous estimates of radial velocities for these objects available in literature are also presented for a comparison. Except for HD 100764 with a radial velocity of about 5 km s⁻¹, the other three are high velocity objects. The heliocentric radial velocities for HD 26, HD 198269 and HD 224959 are respectively +210 km s⁻¹, -200 km s⁻¹ and -126 km s⁻¹.

4 RESULTS

The high-resolution spectra are characterized by closely-spaced lines of carbon bearing molecules of CH, CN and the Swan system of C₂. A few unblended atomic lines were possible to identify only from the regions that are relatively clear of molecular lines. On a line-by-line basis, possible blends between atomic and molecular lines were identified and eliminated and unblended atomic lines were measured from the regions that are relatively clear of molecular lines. Both the CH and the C₂ Swan band systems line lists of Phillips and Davis (1968), the solar atlas, and, the atomic line lists of

Kurucz were used for this purpose. A list of Fe I and Fe II lines considered in the present analysis for the determination of atmospheric parameters and metallicity is given in Table 4.

4.1 Temperature estimates from photometry

Estimates of the effective temperatures of the program stars have been determined using the temperature calibrations derived by Alonso et al. (1996) which relate T_{eff} with various optical and near-IR colours. Using this method Alonso et al. estimate an external uncertainty of $\sim 90\text{K}$ in the temperature calculation. The calibrations of $B - V$, $V - R$, $V - I$, $R - I$ and $V - K$ require colours in the Johnson system, and the calibrations of the IR colours $J - H$, and $J - K$ in the TCS system (the photometric system at the 1.54m Carlos Sanchez telescope in Tenerife; Arribas & Martinez-Roger 1987). To obtain the $V - K$ colour in the Johnson system we first transformed the K_s 2MASS magnitude to the TCS system. Then, using eqs (6) and (7) of Alonso et al. (1994), K is transformed to the Johnson system from the TCS system. In order to transform the 2MASS colours $J - H$ and $J - K_S$ onto the TCS system we first transformed the 2MASS colours to CIT colours (Cutri et al. 2003), and then from CIT to the TCS system (Alonso et al. 1994). Estimation of the T_{eff} from the $T_{\text{eff}} - (J - H)$ and $T_{\text{eff}} - (V - K)$ relations also involves a metallicity ($[\text{Fe}/\text{H}]$) term. We have estimated the T_{eff} of the stars at several metallicities. The estimated temperatures, along with the adopted metallicities, are listed in Table 5. The temperatures span a wide range. In particular, in the case of HD 198269, $J - H$ and $J - K_S$ provide very low temperatures than that given by $V - K$ colour.

5 STELLAR ATMOSPHERIC PARAMETERS

A standard LTE analyses procedure was adopted to determine the stellar atmospheric parameters, the effective temperature (T_{eff}), the surface gravity ($\log g$), and metallicity ($[\text{Fe}/\text{H}]$) of the stars. A recent version of MOOG of Sneden (1973) is used. Model atmospheres are selected from the Kurucz grid of model atmospheres computed with better opacities and abundances with no convective overshooting. These models are available at <http://cfaku5.cfa.harvard.edu/>, labelled with the suffix “odfnew”. The abundance analysis is made using the grid calculated for C-normal chemical composition. The excitation potentials and oscillator strengths of the lines are taken from various sources (Vienna Atomic Line Database (<http://ams.astro.univie.ac.at/vald/>), Kurucz atomic line list (<http://www.cfa.harvard.edu/amp/ampdata/kurucz23/sekur.html>), Fuhr, Martin, & Wiese (1988),

¹ IRAF is distributed by the National Optical Astronomical Observatories, which is operated by the Association for Universities for Research in Astronomy, Inc., under contract to the National Science Foundation

Table 2: Photometric parameters for program and comparison stars

Stars	RA(2000)	Dec(2000)	Sp Ty	V	B - V	R - I	V - I	E(B - V)	J	H	K _s
HD 26	00 05 22.20	+08 47 16.11	K0III/G4Vp	8.22	1.05	-	-	0.05	6.540	6.106	6.032
HD100764	11 35 42.74	-14 35 36.66	CH/R0/R2/C	8.73	1.05	0.51	0.92	0.02	7.048	6.60	6.513
HD198269	20 48 36.74	+17 50 23.72	R0/R	8.12	1.28	0.58	1.14	0.10	6.078	5.505	5.385
HD224959	00 02 08.02	-02 49 12.26	R2/R0	9.55	1.12	0.51	0.96	0.03	7.863	7.432	7.303

The values of B-V, R-I, V-I are taken from Platais et al. 2003, A&A, 397, 997.

Table 3: Heliocentric Radial velocities v_r of the program stars

Stars	HJD	v_r km s ⁻¹		
		Our estimates	from literature	References
HD 26	2452784.95121	+210.5 ± 1.5	-212.9	1
HD 100764	2453157.73074	+4.9 ± 1.5	+5.0	2
HD 198269	2453158.01437	-200.5 ± 1.5	-204.0	3
			-207.0	4
			-203.4	5
HD 224959	2453156.12808	-126.5 ± 1.5	-132.0	4
			-127.8	5

References- 1 : Aoki & Tsuji (1997), 2: Keenan (1993) and Dominy (1984), 3 : Nordstroem, B. et al. (2004), 4: Hartwick & Cowley (1985), 5: McClure & Woodsworth (1990)

Martin, Fuhr, & Wiese (1988), and Lambert et al. 1996, *gf* values of elements compiled by R.E. Luck.

The effective temperature of the stars were obtained by the method of excitation balance, forcing the slope of the abundances from Fe I lines versus excitation potential to be near zero. The temperature estimates derived from JHK photometry (Table 5) provided a preliminary temperature check for choosing an initial model atmosphere. The final effective temperatures were then obtained by an iterative process using the method of excitation balance. A comparison of the effective temperatures derived from photometry and spectroscopy shows that the spectroscopic estimates are closer to temperature estimates obtained from (J-H) relation which are not too different from those obtained from (J-K) relation. HD 198269 is an exception where estimates from (J-K) and (J-H) show significant difference from the spectroscopic value. It is likely that in case of HD 198269 there could be some molecular bands affecting J band. The T_{eff} from (V-K) show a deviation of about 300 K from spectroscopic ones, the estimates from (V-K) is relatively reliable compared to those from optical colours e.g. V-R and B-V. The adopted microturbulence is 2 km s⁻¹ for all the objects. Such a value is not unrealistic; (in cool giants, with $\log g \leq 2.0$, in general $V_t \geq 2$ km s⁻¹ (Vanture 1992c, McWilliam et al. 1995a,b)). The surface gravity of the stars were derived using the Fe I/Fe II ionisation equilibrium. The derived atmospheric parameters T_{eff} , $\log g$, and [Fe/H] of the stars are listed in Table 6. The correctness of our estimates is verified by reproducing the atmospheric parameters obtained by Barbuy et al. (2005) for the star CS 22948-027. Their estimates are very close to our estimates (refer to Goswami et al. (2006), Table 5).

6 ABUNDANCE OF ELEMENTS

The spectra of the program stars are affected severely by line blending. We have used a standard abundance analysis procedure based on the equivalent width measurements only for those elements for which we could measure more than two clean lines. Spectral synthesis method is used for elements for which we could measure only one good line. Local thermodynamic equilibrium is assumed for the spectrum synthesis calculations. We have used

the latest version of MOOG Sneden (1973) for spectrum synthesis. The line list for each region synthesized is taken from the Kurucz atomic line list (<http://www.cfa.harvard.edu/amp/-ampdata/kurucz23/sekur.html>) and from the Vienna Atomic Line Database

(<http://ams.astro.univie.ac.at/vald/>). Reference solar abundances for the various elemental species are adopted from Asplund, Grevesse & Sauval (2005). The $\log gf$ values for atomic lines are also adopted from Fuhr et al. (1988) and Martin et al. (1988), and from a compilation of *gf* values by R. E. Luck (private communication). For heavy neutron-capture elements $\log gf$ values given by Sneden et al. (1996) and Lawler et al. (2001) are consulted. The atomic parameters of the lines used for abundance determination of the elements and their measured equivalent widths are given in appendix (Table 13). The derived elemental abundances of the stars are presented in Tables 7 through 10. In these Tables, we have listed the abundance $\log \epsilon(X)$, along with [X/H] and [X/Fe] values. In computing the quantity [X/Fe] we have used the Fe I-based abundance for elemental abundances derived from neutral lines and the Fe II-based abundance for elemental abundances derived from ionized lines. Elemental abundances are discussed in the following sections.

6.1 Carbon, Nitrogen, Oxygen

The Carbon abundance is derived from spectral synthesis calculation of the G-band of CH around 4315 Å. A synthetic spectrum, derived with an appropriate model atmosphere and using a carbon abundance of $\log \epsilon(C) = 7.7 \pm 0.3$, shows a good match to the depth of the observed spectrum of HD 26. Relative to the solar photospheric C abundance, C is mildly enhanced in HD 26 ($[C/Fe] = +0.31$). Spectrum synthesis calculation also shows Carbon to be strongly enhanced in HD 198269 and HD 224959 with $[C/Fe]$ values of 2.30 and 2.01 respectively. Spectrum synthesis fits of the region 4310 - 4330 Å is shown in Figure 1.

Reported C, N, O overabundances with respect to Fe ($[X(C,N,O)/Fe]$) in HD 26, and HD 224959 (Masseron et al. 2010) are respectively (0.68, 0.94, 0.36), (1.77, 1.88, 1.10). A carbon abundance of $\log \epsilon(C)$ of 7.45 is reported for HD 198269. The Carbon isotopic ratio ($^{12}C/^{13}C = 5$) is same as that of Van-

Table 4: Fe lines used for determination of the atmospheric parameters

W_{lab}	ID	EP_{low}	log gf	HD 100764 Eqw (mÅ)	HD 224959 Eqw (mÅ)	HD 198269 Eqw (mÅ)	HD 26 Eqw (mÅ)
6593.871	Fe I	2.43	-2.42	—	—	75.7	—
6592.910	Fe I	2.72	-1.60	140.5	—	—	—
6518.380	Fe I	2.83	-2.75	78.5	—	—	—
6421.350	Fe I	2.28	-2.03	—	—	111.3	—
6411.650	Fe I	3.65	-0.82	—	34.9	88.9	—
6393.612	Fe I	2.43	-1.62	—	—	135.7	—
6335.340	Fe I	2.19	-2.23	134.0	—	—	—
6252.550	Fe I	2.40	-1.69	154.3	41.7	—	—
6246.317	Fe I	3.60	-0.96	—	—	78.6	—
6230.726	Fe I	2.55	-1.28	190.4	57.6	—	—
6219.279	Fe I	2.20	-2.43	—	—	—	—
6137.694	Fe I	2.58	-1.40	189.0	—	97.8	—
6136.615	Fe I	2.45	-1.40	184.0	53.8	124.6	—
5586.760	Fe I	3.36	-0.21	159.3	58.6	118.0	—
5324.179	Fe I	3.21	-0.10	—	69.3	130.6	152.2
5266.555	Fe I	2.99	-0.49	—	—	—	—
5242.490	Fe I	3.63	-0.84	98.6	—	—	—
5232.939	Fe I	2.94	-0.19	—	82.6	148.3	169.0
5202.340	Fe I	2.18	-1.84	—	47.7	129.7	—
5192.343	Fe I	2.99	-0.52	—	64.8	130.7	—
5171.595	Fe I	1.48	-1.79	—	86.9	156.8	157.6
5166.282	Fe I	0.00	-4.19	—	51.3	150.8	145.2
5051.635	Fe I	0.91	-2.79	—	84.0	157.2	—
5049.819	Fe I	2.27	-1.42	—	—	139.0	—
5012.068	Fe I	0.85	-2.64	—	74.8	169.3	—
5006.119	Fe I	2.83	-0.61	—	71.0	130.4	—
5001.860	Fe I	3.88	+0.009	146.4	32.4	—	100.8
4994.130	Fe I	0.91	-2.96	—	59.7	130.4	129.8
4982.524	Fe I	4.10	+0.14	129.1	—	75.8	—
4966.087	Fe I	3.33	-0.89	—	—	85.6	103.2
4939.690	Fe I	0.85	-3.34	—	—	—	130.0
4938.814	Fe I	2.87	-1.08	—	—	—	100.7
4924.770	Fe I	2.27	-2.25	136.3	—	93.8	99.2
4918.990	Fe I	2.87	-0.34	—	81.6	139.1	148.7
4903.310	Fe I	2.88	-0.93	151.0	46.3	104.6	122.7
4891.490	Fe I	2.85	-0.14	—	—	151.5	179.2
4890.755	Fe I	2.87	-0.39	—	—	—	181.5
4877.610	Fe I	2.99	-3.15	50.1	—	—	—
4871.317	Fe I	2.86	-0.41	—	—	146.4	148.1
4869.450	Fe I	3.54	-2.52	49.2	—	—	—
4834.510	Fe I	2.42	-3.41	70.0	—	—	—
4787.833	Fe I	3.00	-2.77	60.5	—	—	27.0
4632.911	Fe I	1.61	-2.91	—	—	96.5	—
4494.560	Fe I	2.19	-1.14	—	70.7	130.0	—
4491.490	Fe I	2.85	-0.11	—	—	—	—
4489.740	Fe I	0.12	-3.97	—	—	—	134.7
4484.219	Fe I	3.60	-0.72	—	—	67.6	88.5
4476.019	Fe I	2.84	-0.82	—	63.5	—	146.5
4466.552	Fe I	2.83	-0.60	—	—	—	151.6

ture (1992b). Vanture (1992b) has determined oxygen abundance ($\log \epsilon(\text{O})$) for these objects from O I near-infrared triplet near 7774 Å applying non-LTE corrections; these values are ≤ 7.7 for HD 224959, ≤ 7.6 for HD 198269 and 8.45 for HD 26. With respect to Fe, Vanture found carbon to be enhanced by +0.45 (HD 26), +0.91 (HD 198269) and + 1.71 (HD 224959).

No clean oxygen lines are detected in our spectra. We have made a rough estimate of oxygen by considering the fact that, the CH stars for which oxygen abundances have been determined follow a particular trend: Oxygen abundance in halo stars are found to increase with decreasing metallicity as $[\text{O}/\text{Fe}] \sim -0.5 [\text{Fe}/\text{H}]$ until $[\text{Fe}/\text{H}] = -1.0$ and then level off at a value of $[\text{O}/\text{Fe}] = +0.35$

(Wheeler et al. 1989, Goswami & Prantzos 2000). Based on this the Oxygen abundances ($\log \epsilon(\text{O})$) are respectively 7.9 (HD 26), 7.1 (HD 198269), 6.6 (HD 224959) and 9.0 (HD 100764).

6.2 The odd-Z elements Na and Al

Na abundance is calculated from the resonance doublet - Na I D lines at 5890 Å and 5896 Å. These resonance lines are sensitive to non-LTE effects (Baumüller & Gehren 1997; Baumüller et al. 1998; Cayrel et al. 2004). The non-LTE correction could be as high as ± 0.1 dex. The derived abundance $[\text{Na}/\text{Fe}]$ from an

Table 4: (continued)

W_{lab}	ID	EP_{low}	log gf	HD 100764 Eqw (mÅ)	HD 224959 Eqw (mÅ)	HD 198269 Eqw (mÅ)	HD 26 Eqw (mÅ)
4447.720	Fe I	2.22	-1.34	—	—	—	—
4443.190	Fe I	2.86	-1.04	—	50.0	—	—
4256.790	Fe I	4.25	-1.56	45.1	—	—	—
6456.390	Fe II	3.90	-2.07	—	—	43.2	—
5234.625	Fe II	3.22	-2.05	111.4	37.5	73.9	99.6
5197.559	Fe II	3.23	-2.10	106.6	48.5	76.8	—
4993.350	Fe II	2.81	-3.67	—	—	—	51.5
4923.930	Fe II	2.89	-1.32	—	85.8	135.6	167.8
4731.440	Fe II	2.89	-3.36	—	—	—	—
4620.510	Fe II	2.83	-3.29	—	—	—	84.4
4583.839	Fe II	2.80	-2.02	—	72.6	106.5	—
4576.330	Fe II	2.84	-3.04	92.1	—	—	—
4520.230	Fe II	2.81	-2.60	—	58.4	—	—
4515.340	Fe II	2.84	-2.48	—	29.7	67.9	—
4508.280	Fe II	2.85	-2.21	—	44.3	78.6	—
4491.400	Fe II	2.85	-2.70	—	27.9	59.2	—

Table 5: Effective temperatures from Photometry

Star Name	V	J	H	K	T_{eff} (K) (J-K)	T_{eff} (K) (J-H)	T_{eff} (K) (V-K)	T_{eff} (K) Spectroscopy
HD 26	8.22	6.540	6.106	6.032	5112.4	4957.8(-0.5)	4811.3(-0.5)	5000
						4974.5(-1.0)	4798.7(-1.0)	
						4991.3(-1.5)	4790.7(-1.5)	
						5008.3(-2.0)	4787.3(-2.0)	
						5025.3(-2.5)	4788.5(-2.5)	
HD 100764	8.73	7.048	6.600	6.153	3849.9	4990.9(-0.5)	4394.8(-0.5)	4750
						5007.6(-1.0)	4378.6(-1.0)	
						5024.4(-1.5)	4366.2(-1.5)	
						5041.3(-2.0)	4357.6(-2.0)	
						5058.3(-2.5)	4352.8(-2.5)	
HD 198269	8.12	6.708	5.505	5.385	2979.5	2610.1(-0.5)	4245.6(-0.5)	4500
						2622.7(-1.0)	4228.3(-1.0)	
						2635.3(-1.5)	4214.6(-1.5)	
						2648.1(-2.0)	4204.5(-2.0)	
						2660.9(-2.5)	4197.9(-2.5)	
HD 224959	9.55	7.863	7.432	7.303	4902.6	4988.6(-0.5)	4744.1(-0.5)	5000
						5005.3(-1.0)	4730.8(-1.0)	
						5022.1(-1.5)	4722.1(-1.5)	
						5038.9(-2.0)	4717.7(-2.0)	
						5056.0(-2.5)	4717.8(-2.5)	

The numbers in the parenthesis indicate metallicities.

LTE analysis are +0.29 (HD 26), +0.16 (HD 224959) and +0.20 (HD 198269). HD 26 gives [Na/Fe] in marginal excess of the First Dredge Up (FDU) predictions of El Eid & Champagne (1995) ([Na/Fe] of +0.18 for a 5 M_{\odot} stellar model. Enrichment of Na is believed to result from mixing of products of Ne-Na cycle involving proton-capture on ^{22}Ne in H burning region, following first dredge up.

Al lines in our spectral coverage are severely blended and could not be used for abundance determination.

6.3 The α -elements Mg, Si, Ca, Ti

Magnesium (Mg): The Mg abundance is derived from the synthesis of the Mg I line at 5172.68 Å. The predicted line profile with our adopted Mg abundances fits the observed line profile quite well. **We have also measured the Mg abundance using lines at 4057.500, 4571.100 and 5528.400 Å. The pre-**

sented abundance ratios in the Tables 7 - 10 are an average of the abundances derived from these four lines. Magnesium is found to exhibit an overabundance with [Mg/Fe] \sim +0.56 in HD 26. For HD 198269 and HD 224959 we have obtained [Mg/Fe] = +0.41 and +0.25 respectively.

Silicon (Si): Lines of Si detected in the spectra of these objects are severely blended and could not be used for abundance determination.

Calcium (Ca): Abundance of Ca is derived using three lines of Ca I at 6102.72, 6122.22 and 6439.07 Å for HD 26. Eight lines for HD 198269 and four for HD 224959 are used to derive Ca abundance. The derived abundance estimates are respectively [Ca/Fe] = +0.24 (HD 26), +0.52 (HD 198269) and +0.40 (HD 224959). Estimated Non-LTE corrections for abundances derived from Ca I line for dwarfs and subgiants is about +0.1 dex. Hence we do not expect a large change in our estimates of [Ca/Fe] caused by Non-LTE effect. Abundance of Ca could not be estimated for HD 100764 from our spectrum.

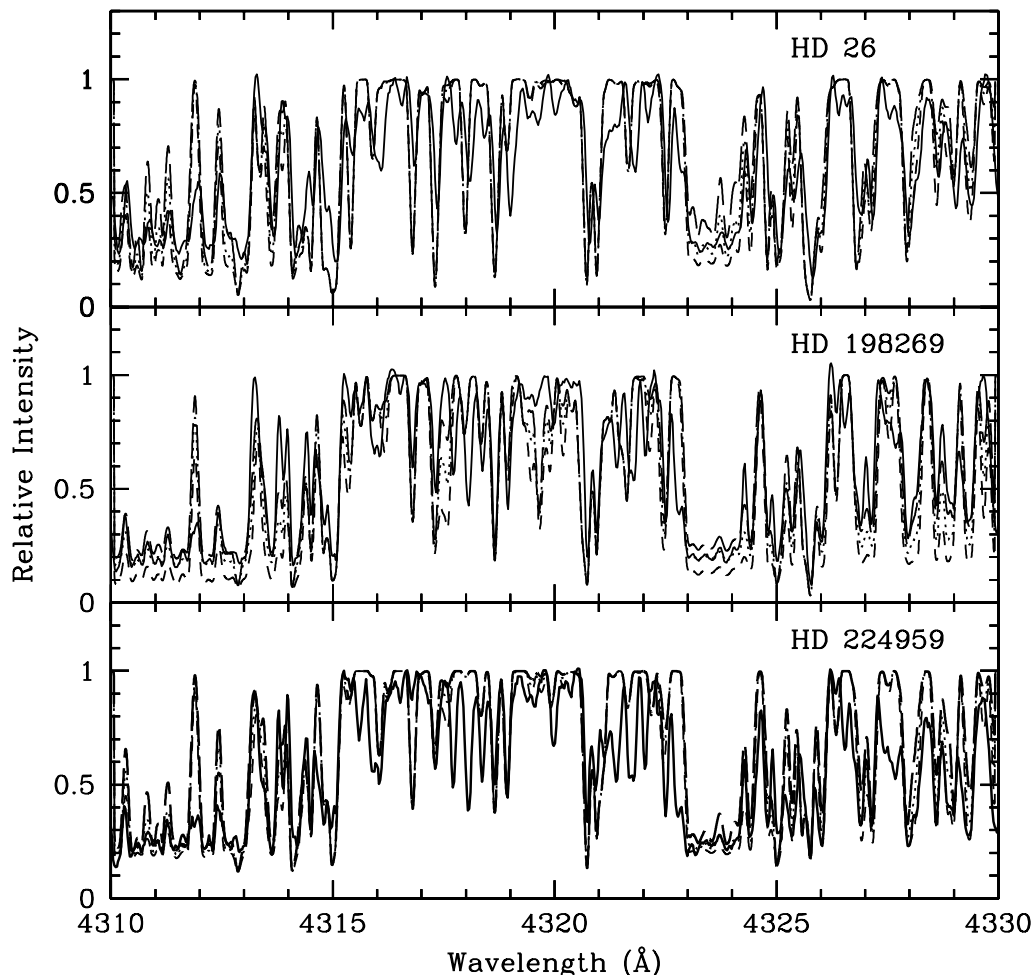


Figure 1. Spectrum synthesis fits of the region 4310 - 4330 Å (dotted curve) compared with the observed spectra (solid curve) of HD 26 (top panel). Spectrum synthesis fits for HD 198269 and HD 224959 are shown in the middle and the bottom panel respectively. The synthetic spectra are obtained using a model atmosphere corresponding to the adopted parameters listed in Table 6. Two alternative synthetic spectra for $\Delta[X/Fe] = +0.3$ (long dash) and $\Delta[X/Fe] = -0.3$ (dot-dash) are shown to demonstrate the sensitivity of the line strength to the abundances.

Scandium (Sc): Spectrum synthesis of Sc II line at 6245.63 Å considering hyperfine structure from Prochaska and McWilliam (2000) gave $[Sc/Fe] = 0.52$ for HD 198269, $[Sc/Fe] = -0.20$ for HD 26, and $[Sc/Fe] = -0.89$ for HD 224959. Spectrum synthesis plots are shown in Figure 2. Sc II line at 5031.02 Å could be measured only for the star HD 198269. Due to the presence of C₂ lines in this region, estimates of Sc abundance using this line would likely to return inaccurate estimate.

Titanium (Ti): The abundance of Ti derived from Ti I and Ti II lines differ slightly. For HD 26, two Ti I lines at 4533.24 and 4534.77 Å and four Ti II lines at 4418.33, 4443.794, 4563.77 and 4865.61 Å are used. Log gf values are taken from Kurucz data base. Abundances with respect to Fe ($[Ti I/Fe]$ and $[Ti II/Fe]$) are respectively -0.06 , $+0.17$ in HD 26, 0.22 and 0.48 in HD 198269, and 0.44 , 0.49 in HD 224959. The number of Ti I and Ti II lines used for the calculations are four and eight respectively for HD 224959 and seven and thirteen respectively for HD 198269. Non-LTE correction for the abundance of Ti derived from Ti I is about $+0.1$ dex for dwarf and subgiants. If we consider this correction factor the difference between the abundances derived

from Ti I and Ti II lines will reduce at most by 0.1 dex and the abundances obtained from Ti I and Ti II lines of HD 224959 would be almost similar. No lines of Ti were found usable to derive Ti abundance for HD 100764.

6.4 The iron-peak elements V, Cr, Mn, Ni, Zn

Vanadium (V): Abundance of V in HD 198269 is estimated from spectrum synthesis calculation of V I line at 5727.028 Å taking into account the hyperfine components from Kurucz database that gives $[V/Fe] = +0.13$. This line could not be detected in HD 26 and HD 224959.

Chromium (Cr): The Cr abundance derived using four Cr I lines give $[Cr/Fe] = -0.13$ for HD 198269. The Cr abundance derived from a single Cr I line at 4626.19 Å returns a $[Cr/Fe]$ value of -0.19 for HD 26. Estimates of $[Cr/Fe]$ for HD 198269 and HD 224959 are respectively -0.08 (five lines) and -0.24 (two lines).

Manganese (Mn): The Mn abundance is derived from three Mn I lines for HD 198269 give $[Mn/Fe] = -0.13$. No clear good

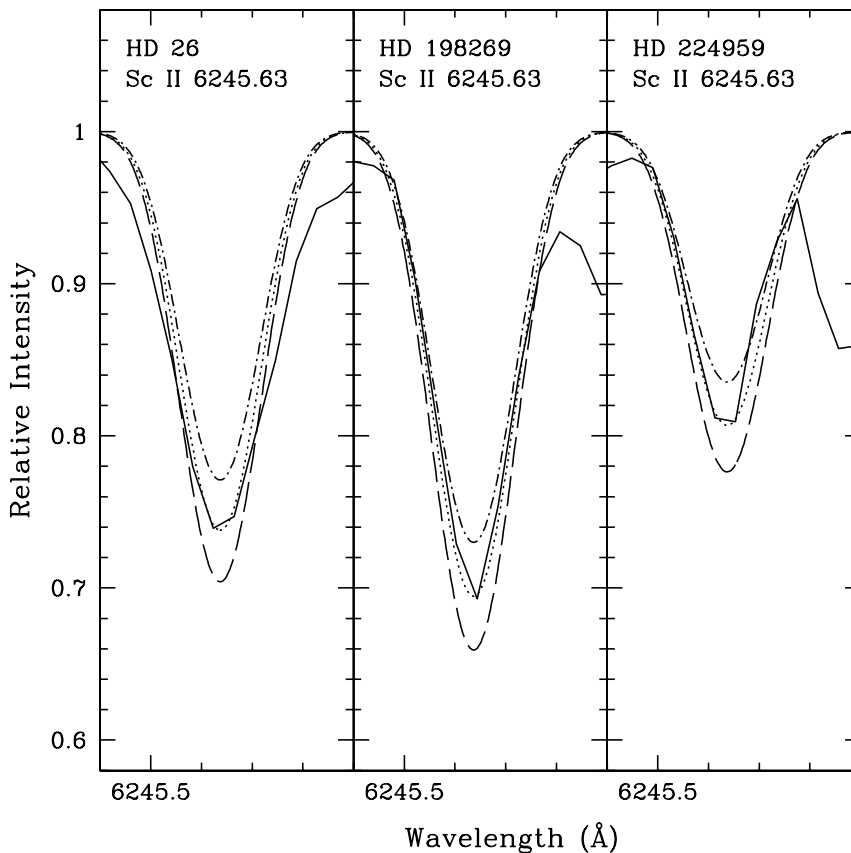


Figure 2. Spectrum synthesis fits of Sc (dotted curve) compared with the observed spectra (solid curve) of HD 26, HD 198269 and HD 224959. The synthetic spectra are obtained using a model atmosphere corresponding to the adopted parameters listed in Table 6. Two alternative synthetic spectra for $\Delta[X/Fe] = +0.1$ (long dash) and $\Delta[X/Fe] = -0.1$ (dot-dash) are shown to demonstrate the sensitivity of the line strength to the abundances.

lines due to Mn are detected in the spectra of HD 26, HD 224959 and HD 100764. The abundance of Mn derived using spectrum synthesis calculation of Mn I line at 6013.51 Å line taking account of hyperfine structures from Prochaska and McWilliam (2000) returns a value $[Mn/Fe] = -0.13$ for HD 198269. This value for HD 26 is found to be -0.23 . The Mn I line at 6013.51 Å could not be detected in HD 224959.

Nickel (Ni): Abundance of Ni in HD 26 is derived from two Ni I lines at 4980.16 Å and 5035.36 Å. Derived $[Ni/Fe] = -0.06$. We could use only one good line of Ni I to derive its abundance in HD 224959. $[Ni/Fe]$ is found to be 0.09. For HD 198269 we have used five lines of Ni I and derived a value -0.01 for $[Ni/Fe]$.

Zinc (Zn): The Zn abundance is derived from a single Zn I line at 4810.53 Å in HD 26. $[Zn/Fe]$ for HD 26 is found to be solar. No clear good lines could be detected in the spectra of HD 198269 and HD 224959. Estimated $[Zn/Fe]$ is 0.11 for HD 100764.

6.5 The light s-process elements Sr, Y, and Zr

Strontium (Sr): The Sr abundance is derived from Sr I line at 4607.327 Å. Sr shows an overabundance ($[Sr/Fe]$) of 1.89 for HD 26, 1.06 for HD 198269 and 1.50 for HD 224959. Sr II lines at 4077.7 Å and 4215.52 Å are blended, the latter with contributions from the CN molecular band around 4215 Å. Sr II line at 4161.82 Å could not be detected in the spectra of these objects. Sr I line at 6550.24 Å is blended with a Sc II line and therefore not

used for abundance calculation. Sr abundance in HD 100764 could not be estimated; the spectral synthesis calculation of 4607.327 Å line did not give an acceptable synthetic fit with the observed feature in HD 100764.

Yttrium (Y): The abundance of Y with respect to Fe shows an overabundance ($[Y/Fe]$) of 0.89 in HD 26, and 0.22 in both HD 198269 and HD 224959. Among several lines of Y II examined in the spectra of these objects, Y II 5200.41 Å line appears as a good line. Y II line at 5205.73 Å is also detected as a shallow feature. The line at 4398.1 Å is asymmetric on the right wing, probably blended with a Nd II line at 4398.013 Å and could not be used for abundance determination. Y II line at 4883.69 Å is also asymmetric on the right wing, blended with a Sm I line at 4883.777 Å. Y II line at 5087.43 Å shows asymmetry on the right wing, and 5123.22 Å line appears as a shallow feature, both the wings not reaching the continuum. Y I line at 4982.129 Å is blended with a Mn I line. The line at 5473.388 Å is blended with contributions from Mo I and Ce I lines. Spectral synthesis calculation of Y II line at 5200.41 Å returns a near-solar value for HD 100764 with $[Y/Fe] = -0.08$.

Zirconium (Zr): The abundance of Zr is derived using a single Zr II line at 4317.321 Å. Zr shows an overabundance with $[Zr/Fe]$ of 1.16 for HD 26. Spectral synthesis of Zr I line at 6134.57 Å which is weakly detected in the spectrum of HD 26 did not give a good synthetic fit with the observed feature and returned a value of $[Zr/Fe] = 1.16$. None of the Zr I lines are usable for abundance determination. Zr II line at 4496.97 Å appears as a

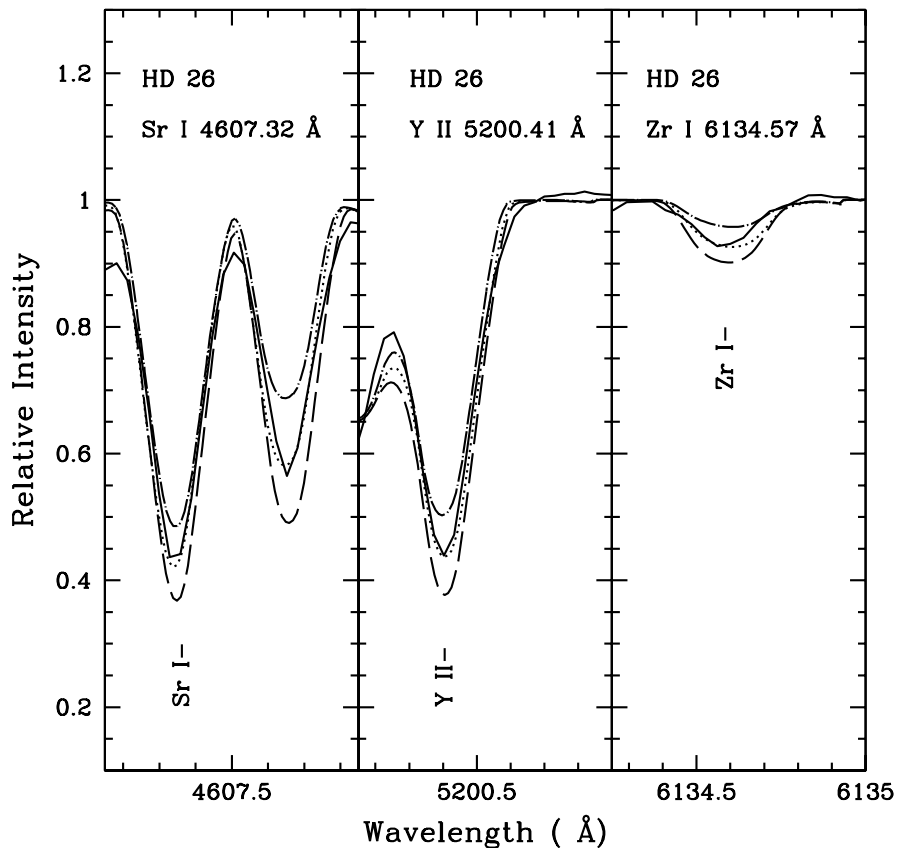


Figure 3. Spectrum synthesis fits of Sr, Y and Zr (dotted curve) compared with the observed spectra (solid curve) of HD 26. The synthetic spectra are obtained using a model atmosphere corresponding to the adopted parameters listed in Table 5. Two alternative synthetic spectra for $\Delta[\text{Sr}, \text{Y}, \text{Zr}/\text{Fe}] = +0.3$ (long dash) and $\Delta[\text{Sr}, \text{Y}, \text{Zr}/\text{Fe}] = -0.3$ (dot-dash) are shown to demonstrate the sensitivity of the line strength to the abundances.

blend with Co I line at 4496.911 Å. Absorption tip of Zr II line at 4161.21 is easily detected. Lines detected at 4208.99, 4258.05 and 4317.32 Å are heavily contaminated by contributions from molecular bands. Zr II line at 4404.75 Å is blended with an Fe I line and the 4317.321 Å line is blended with a Ce II line. Spectrum synthesis fits of Sr, Y and Zr are shown in Figure 3 for HD 26. Abundance of Zr could not be estimated for HD 100764 as no clean lines of Zr could be detected in its spectrum.

6.6 The heavy n -capture elements: Ba, La, Ce, Pr, Nd, Sm, Eu, Er, W, Pb

The abundances of the heavy n -capture elements barium (Ba), lanthanum (La), cerium (Ce), neodymium (Nd), samarium (Sm), praseodymium (Pr), europium (Eu), erbium (Er), tungsten (W) and lead (Pb) with respect to Fe are generally found to be over-abundant. As the abundances derived from weak lines are not expected to be affected by hyperfine splitting (McWilliam et al. 1995a, b), we have not used hyperfine-splitting corrections for Y, Ce, and Nd lines.

Barium (Ba): The Ba II line at 6141.727 Å is used to determine the Ba abundance in HD 26. Compared to the other barium lines detected in the spectra this line appeared as a well defined symmetric line in all the three CH stars spectra. $\log gf$ value for this line is taken from Miles and Wiese (1966). We have derived $[\text{Ba}/\text{Fe}] = 1.93$ for HD 26. Barium abundance determined using

the lines at 5853.67, 6141.71 and 6496.90 Å returns a value 1.24 for $[\text{Ba}/\text{Fe}]$. The lines used for HD 224959 are 4934.08, 5853.67 and 6171.73 Å; these lines return a value with $[\text{Ba}/\text{Fe}] = 2.07$ for this object. Abundance of Ba is found to be near-solar with $[\text{Ba}/\text{Fe}] = -0.02$ for HD 100764, using the spectrum synthesis calculation of 6141.727 Å. Literature values of Ba abundance for these objects are not available. The spectrum synthesis fits of Ba feature at 6141.7 Å is shown in Figure 4. Abundance of barium derived using spectrum synthesis calculation using Ba II line at 5853.668 Å considering hyperfine components from McWilliam (1998) gave $[\text{Ba}/\text{Fe}] = 2.75$ for HD 224959, higher than what is obtained from 6141.7 Å line. This line could not be used for HD 26.

Lanthanum (La): Three good lines of La are used for HD 26, two for HD 196289 and HD 100764 each, and four for HD 224959 to derive La abundances. La exhibits an overabundance ($[\text{La}/\text{Fe}]$) of 1.53 in HD 26, 1.57 in HD 198269, 0.83 in HD 100764, and 2.50 in HD 224959. Our estimate of $[\text{La}/\text{Fe}]$ matches closely with those of Van Eck et al. and Vanture for HD 224959 and HD 198269. For HD 26, our estimate ($[\text{La}/\text{Fe}] = 1.56$) is closer to Vanture's ($[\text{La}/\text{Fe}] = 1.4$), but about 0.8 dex lower than that given by Van Eck et al. ($[\text{La}/\text{Fe}] = 2.3$). No previous estimate ($[\text{La}/\text{Fe}]$) for HD 100764 is available for a comparison. Spectrum synthesis calculation of La II line at 4921.77 Å (shown in Figure 5) considering hyperfine components from Jonsell et al. (2006) give $[\text{La II}/\text{Fe}] = 1.0$ for HD 26, 1.66 for HD 198269 and 2.6 for HD 224959.

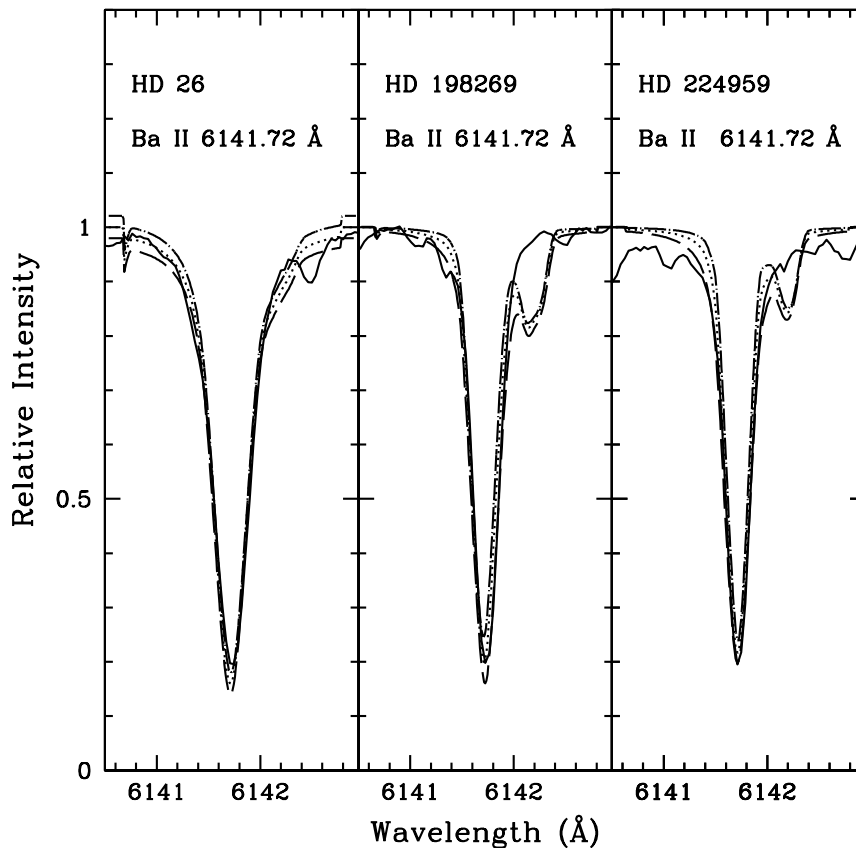


Figure 4. Spectrum synthesis fits of Ba (dotted curve) compared with the observed spectra (solid curve) of HD 26, HD 198269 and HD 224959. The synthetic spectra are obtained using a model atmosphere corresponding to the adopted parameters listed in Table 5. Two alternative synthetic spectra for $\Delta [\text{Ba}/\text{Fe}] = +0.3$ (long dash) and $\Delta [\text{Ba}/\text{Fe}] = -0.3$ (dot-dash) are shown to demonstrate the sensitivity of the line strength to the abundances.

Cerium (Ce): We have examined five Ce I lines and thirty three Ce II lines in our spectra. A few of them are either affected by molecular contamination or blended with contributions from other elements. The abundances of Ce are derived using seven good lines of Ce II for HD 26, twenty one for HD 198269 and seventeen for HD 224959. An overabundance ($[\text{Ce}/\text{Fe}]$) of 1.65 is estimated for HD 26. This value agrees well with that of Van Eck et al. and 0.28 dex lower than that of Vanture's. Our estimated $[\text{Ce}/\text{Fe}]$ for HD 198269 ~ 1.66 is same as that obtained by Vanture (1992c) and 0.1 dex higher than the estimate of Van Eck et al. Our estimated $[\text{Ce}/\text{Fe}] \sim 2.28$ for HD 224959 is about 0.3 dex higher than that of Van Eck et al. and 0.15 dex higher than that of Vanture's estimate. We have derived $[\text{Ce}/\text{Fe}] = 1.66$ for HD 100764 using seven good Ce II lines. No previous estimate of $[\text{Ce}/\text{Fe}]$ is available for this object.

Praseodymium (Pr): The abundance of Pr is derived using four good lines each for HD 26 and HD 224959, and five lines are used for HD 198269. Pr exhibits an overabundance with $[\text{Pr}/\text{Fe}] = +1.64$ in HD 26, 1.49 in HD 198269 and 2.35 in HD 224959. Literature values of Pr abundance for these objects are not available. Among the one Pr I line and eight Pr II lines examined in our spectra, Pr I line at 5996.060 Å is detected as an asymmetric line. Pr II line at 5188.217 Å is blended with a La II line and lines at 5219.045 Å and 5220.108 Å appeared as asymmetric lines. As none of the Pr lines detected in the spectrum of HD 100764 is usable for the abundance analysis, Pr abundance could not be estimated for HD 100764.

Neodymium (Nd): One Nd I and thirty six Nd II lines listed in Table 13 are examined. Most of them are blended with contributions from other elements. Twelve good lines of Nd II are used for HD 26, twenty one for HD 198269 and twenty for HD 224959 to derive abundance of Nd in these objects. Neodymium shows an overabundance with $[\text{Nd}/\text{Fe}] = 1.45$ for HD 26. This value agrees with that given by Vanture (1992c) but higher by 0.15 dex than that estimated by Van Eck et al. (2003). Luck & Bond (1982) estimated $[\text{Nd}/\text{Fe}] = 1.99$ for this object. $[\text{Nd}/\text{Fe}] = 2.30$ obtained for HD 224959 and $[\text{Nd}/\text{Fe}] = 1.48$ obtained for HD 198269 are about 0.25 dex higher those of Van Eck et al. (2003) and 0.45 dex higher than that of Vanture (1992c). Abundance of Nd derived from a single line shows an overabundance with $[\text{Nd}/\text{Fe}] = 1.08$ for HD 100764.

Samarium (Sm): Two Sm I and eighteen Sm II lines have been examined in the spectra of these objects. The abundance of Sm is derived using five Sm II lines for HD 26, seventeen for HD 198269 and eleven for HD 224959. Estimated overabundance with $[\text{Sm}/\text{Fe}] = 1.88$ for HD 26 is 0.6 dex higher than that of Van Eck et al. (2003) but matches well with that of Vanture's estimate. Luck & Bond (1982) gave a much lower value of $[\text{Sm}/\text{Fe}] = 0.4$ for this object. In case of HD 198269 and 224959 our estimates are higher than those of both Van Eck et al. and Vanture (Table 11). Abundance of Sm could not be derived for HD 100764. One Sm I and two Sm II lines detected in the spectrum of HD 100764 are not usable for abundance determination.

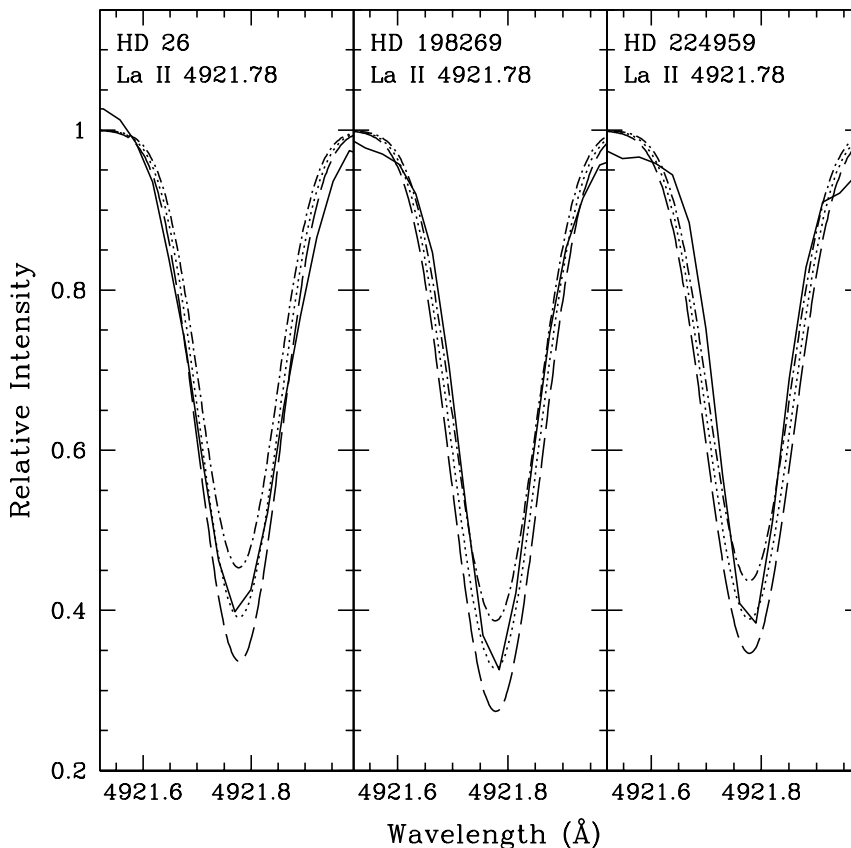


Figure 5. Spectrum synthesis fits of La (dotted curve) compared with the observed spectra (solid curve) of HD 26, HD 198269 and HD 224959. The synthetic spectra are obtained using a model atmosphere corresponding to the adopted parameters listed in Table 6. Two alternative synthetic spectra for $\Delta [\text{La}/\text{Fe}] = +0.3$ (long dash) and $\Delta [\text{La}/\text{Fe}] = -0.3$ (dot-dash) are shown to demonstrate the sensitivity of the line strength to the abundances.

Europium (Eu): The abundance of Eu is determined for HD 26 and HD 224959 from a single good line at 6437.64 Å using spectral synthesis calculation. Eu is overabundant ($[\text{Eu}/\text{Fe}]$) with 0.61 for HD 26 and 2.01 for HD 224959. Previous estimates of Eu in these objects are not available. We could not estimate Eu abundance for HD 100764 and HD 198269 from our spectra as no clean lines could be detected. Spectrum synthesis calculation of 6437.64 Å line did not give good synthetic fits. The blue Eu II lines at 4129.7 and 4205.05 Å and the line at 6645.13 Å are severely blended with strong molecular features and could not be used for abundance analysis.

Erbium (Er): The abundance of Er is estimated using Er II line at 4759.671 Å. The line parameters adopted from Kurucz atomic line list come from Meggers et al. (1975). Er shows an overabundance ($[\text{Er}/\text{Fe}]$) of 1.44 in HD 26, and 1.55 in HD 198269. Er abundance could not be determined for HD 224959 and HD 100764 from our spectra. Er II line at 4820.354 Å is blended with Ti II line at 4820.368 Å.

Tungsten (W): The abundance of W is determined using the W I line at 4757.542 Å. The line parameters taken from the Kurucz atomic line list come from Obbarius and Kock (1982). The abundance derived is high with $[\text{W}/\text{Fe}] = 3.43$ for HD 26 and 2.75 for HD 198269; there is a possible blend with Cr I line at 4757.578 Å (with log g and lower excitation potential, -0.920 and 3.55 respectively) resulting in an overestimate of W abundance. For HD 224959 and 100764 abundance of W could not be estimated from our spectra.

Osmium (Os): Three lines of Os I are detected. Os I at 4048.054 Å is detected in the spectra of all the three stars, HD 26, HD 198269 and HD 224959. However, this line has a possible blend with Cr II line at 4048.025 Å and could not be used for abundance estimates. The other two lines at 4793.996 Å and 4865.607 Å could be detected only in the spectrum of HD 198269. These two lines are blended with Ca I line at 4794.015 Å and Ti II line at 4865.612 Å respectively. The line at 4793.996 Å returns a value showing enhancement with $[\text{Os}/\text{Fe}] = 1.67$ in HD 198269.

Lead (Pb): Spectrum-synthesis calculation is also used to determine the abundance of Pb using the Pb I line at 4057.8 Å. Pb shows an overabundance ($[\text{Pb}/\text{Fe}]$) of 2.11 for HD 26, 2.4 for HD 198269 and 3.70 for HD 224959. This line is strongly affected by molecular absorption of CH. CH lines are included in our spectrum synthesis calculation. This line could not be detected in the spectrum of HD 100764. Our estimated $[\text{Pb}/\text{Fe}]$ for HD 198269 is similar to the estimate of Van Eck et al. 2003. For HD 26 and HD 224959 our estimated $[\text{Pb}/\text{Fe}]$ is about 0.5 dex higher than that obtained by Van Eck et al.. The spectrum synthesis fits of the lead feature is shown in Figure 6 for HD 224959.

6.7 Error Analysis

Error analysis is discussed in detail in one of our earlier paper Goswami et al. (2006). Here we mention it briefly. Random errors and systemic errors are the two main sources of errors affecting

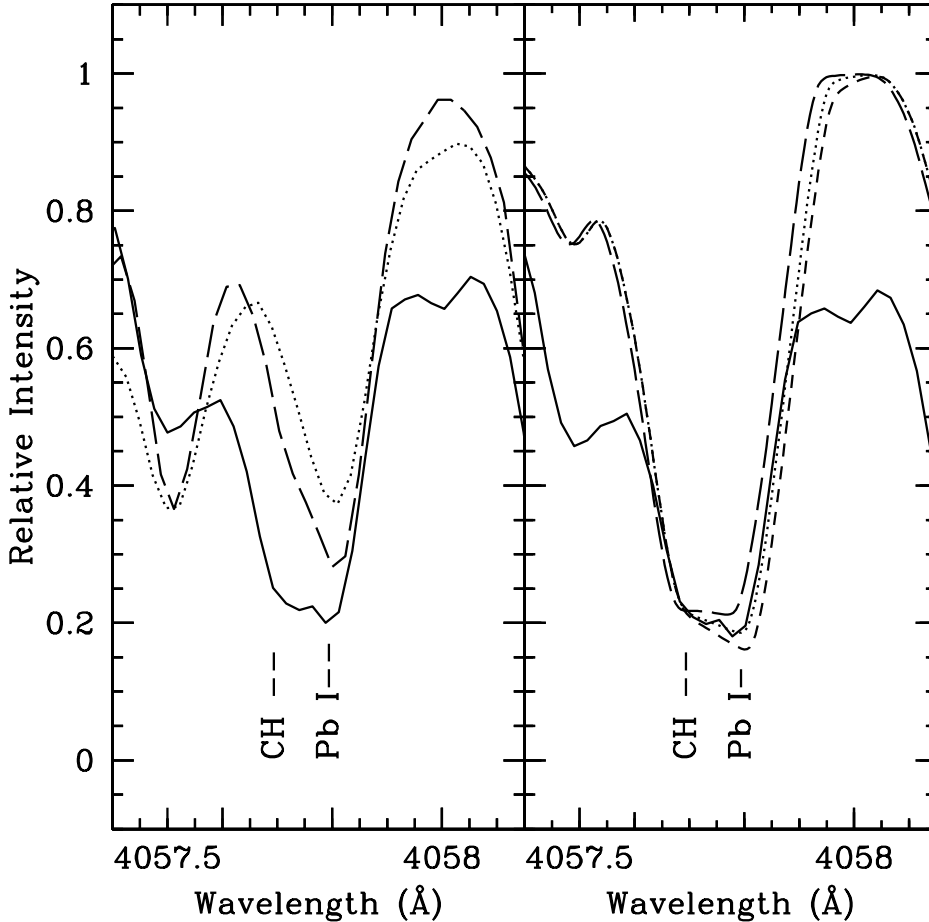


Figure 6. In the left panel the region around the lead feature at 4057.8 Å is compared in the spectrum of HD 26 (dotted line), HD 198269 (dashed line) and HD 224959 (solid line). In the right panel, the spectrum synthesis fits of Pb (dotted curve) is shown with the observed spectra of HD 224959. The synthetic spectra are obtained using a model atmosphere corresponding to the adopted parameters listed in Table 6. Two alternative synthetic spectra for Δ [Pb/Fe] = +0.3 (long dash) and Δ [Pb/Fe] = -0.3 (dot-dash) are shown to demonstrate the sensitivity of the line strength to the abundances.

the derived abundances. Random errors arise due to uncertainties in line parameters, i.e. the adopted gf values and the equivalent width measurements. These errors cause line-to-line scatter in derived abundances for a given species. Random errors are minimized by employing as many usable lines as possible for a given element. In deriving the Fe abundances we made use of Twenty two Fe I lines and four Fe II lines in HD 26, twenty nine Fe I lines and eight Fe II lines in HD 198269 and twenty five Fe I lines and 9 Fe II lines in HD 224959. For the object HD 100764 we could use nineteen Fe I and three Fe II lines. The derived standard deviation σ is defined by $\sigma^2 = [\Sigma(\chi_i - \chi)^2 / (N - 1)]$, where N is the number of lines used. The values of σ computed from the Fe I lines are respectively ± 0.24 , 0.15, 0.24 and 0.27. dex in HD 26, 198269, 224959 and 100764. The corresponding value calculated for Fe II lines are respectively ± 0.18 , 0.13, 0.27 and 0.13. The computed errors for Fe I and Fe II are listed in the Tables 7 - 10.

We have calculated the error in the atmospheric parameters as described by Ryan et al. (1996). The error in the atmospheric parameters have contributions from the measurement of equivalent widths and inaccurate log gf values of Fe lines used for the analysis. Since we have used the most updated log gf values as given in Table 13, the contribution to the error from these values are negligible. To find the minimum error in the atmospheric

parameters, we have used the standard deviation of the Fe abundance derived for each objects as listed in Table 7-10, which is found to be approximately 0.2 dex in all the objects. Along with this corresponding to 0.2 dex in abundance we have calculated the minimum error in the temperature as 100 K, log g as 0.03 and 0.06 km s^{-1} in micro turbulent velocity. Then the minimum contribution from the stellar atmospheric parameters to the elemental abundances are calculated using the general equation

$$E_r = \sqrt{E_{r1}^2 + E_{r2}^2 + E_{r3}^2 + E_{r4}^2 + E_{r5}^2 \dots + E_{rn}^2}$$

The values are found to be 0.25, 0.16, 0.25 and 0.29 in HD 26, HD 198269, HD 224959 and HD 100764 respectively.

For abundances derived by spectrum synthesis calculations we have visually estimated the fitting errors. The estimated fitting errors range between 0.1 dex and 0.3 dex. We adopt these fitting errors as estimates of the random errors associated with the derived elemental abundances.

7 PARAMETRIC MODEL BASED ANALYSIS OF THE OBSERVED ABUNDANCES

We have examined the relative contributions from the s- and r-process to the observed abundances by comparing the observed abundances with predicted s- and r-process contributions in the framework of a parametric model for s-process (Howard et al. 1986). We have used the solar system isotopic abundances (both s- and r-process) given in Arlandini et al. (1999). The solar system r- and s- process elemental abundances derived from the isotopic abundances are scaled to the metallicity of the star. These values are normalized to the observed Ba abundance of the corresponding stars. Using a parametric model function $N_i(Z) = A_s N_{s,i} + A_r N_{r,i}$,

where Z is the metallicity and $N_{s,i}$ and $N_{r,i}$ are the i th element abundance produced respectively by s-process and r-process. The coefficients A_s and A_r that represent the contributions coming from s- and r-process respectively are obtained from non-linear least square fits. The contributions of r- and s-process elements are estimated from the fitting for Ba-Eu. The 1st peak elements Sr, Y and Zr are not included in the fitting as they are not abundantly produced as 2nd peak ones by the s-process in metal-poor AGB stars in general. The model fits are shown in Figure 7. The derived coefficients A_s , A_r and the reduced chisquare (χ^2_ν) values for HD 26, 198269 and 224959 are listed in Table 12.

Table 6: Derived atmospheric parameters

Star Names	T_{eff} (K)	log g	V_t km s $^{-1}$	[Fe I/H]	[Fe II/H]	Remarks
HD 26	5000	1.6	2.07	-1.11	-1.15	1
	5170	2.2		-0.4	-0.4	2
				-0.3	-0.3	4
				-1.25±0.3	-1.25±0.3	4
				-0.45±0.4	-0.45±0.4	5
				-0.45±0.4	-0.45±0.4	6
	5250	2.5	-0.45		10	
HD 100764	4750	2.0	2.0	-0.82	-0.90	1
	4600					7
	4850					8
	4850	2.2	5.0	-0.6		9
HD 198269	4500	1.5	2.25	-2.03	-2.05	1
	4520					8
	4800	1.3			2	
				-2.2±0.2	-2.2±0.2	5
				-1.4	-1.4	4
4460			-1.56		11	
HD 224959	5050	2.1	2.0	-2.42	-2.42	1
	5200	1.9		-1.6		2, 4
				-2.2±0.2	-2.2±0.2	5
				-1.6	-1.4	4

References: 1: this work, 2: Vanture (1992a), 3: Vanture (1992b), 4: Vanture (1992c),
5: Van Eck et al. (2003), 6: Luck & Bond (1982), 7: Bergeat et al. (2001)
8: Aoki & Tsuji (1997), 9: Dominy, J. F. (1984)
10: Smith, V. V. & Lambert, D. L. (1986); 11: Lee P., (1974)

Table 7 : Elemental abundances in HD 26

	Z	solar $\log\epsilon^a$	$\log\epsilon$	[X/H]	[X/Fe]
C	6	8.39	7.7	-0.69	+0.31
N	7	7.78	7.9 ^b	-0.02	+1.12
O	8	8.66	7.9	-0.76	+0.34
Na I	11	6.17	5.35	-0.82	+0.29
Mg I	12	7.53	6.98	-0.55	+0.56
Ca I	20	6.31	6.44±0.11(3)	-0.87	+0.24
Ti I	22	4.90	3.73±0.06(2)	-1.17	-0.06
Ti II	22	4.90	3.96±0.30(4)	-0.94	+0.17
Cr I	24	5.64	4.34(1)	-1.30	-0.19
Mn I	25	5.39	4.05(1)	-1.34	-0.23
Fe I	26	7.45	6.34±0.21(20)	-1.11	-
Fe II	26	7.45	6.30±0.16(4)	-1.15	-
Ni I	28	6.23	5.06(1)	-1.17	-0.06
Zn I	30	4.60	3.49(1)	-1.11	0.0
Sr I	38	2.92	3.7(1)	+0.78	+1.89
Y II	39	2.21	1.95(1)	-0.26	+0.89
Zr I	40	2.59	-	-	-
Zr II	40	2.59	2.6(1)	+0.01	+1.16
Ba II	56	2.17	2.95(1)	+0.78	+1.93
La II	57	1.13	1.51±0.05(3)	+0.38	+1.53
Ce II	58	1.58	2.08±0.13(5)	+0.50	+1.65
Pr II	59	0.71	1.20±0.17(4)	+0.49	+1.64
Nd II	60	1.45	1.75±0.10(8)	+0.30	+1.45
Sm II	62	1.01	1.74±0.30(5)	+0.73	+1.88
Eu II	63	0.52	0.1(1)	-0.42	+0.61
Er I	68	0.93	-	-	-
Er II	68	0.93	1.22(1)	+0.29	+1.44
W I:	74	1.11	3.50(1)	+2.39	+3.54
Pb	82	2.00	3.0(1)	+1.0	+2.11

^a Asplund et al. (2005), ^b Vanture (1992b)

Numbers within parenthesis in column 4 indicate the number of lines used for abundance estimate.

Table 8 : Elemental abundances in HD 100764

	Z	solar $\log\epsilon^a$	$\log\epsilon$	[X/H]	[X/Fe]
Fe I	26	7.45	6.63±0.27(19)	-0.82	-
Fe II	26	7.45	6.55±0.13(3)	-0.90	-
Zn	30	4.60	2.21(1)	-0.71	+0.11
Y II	39	2.21	1.23(1)	-0.98	-0.08
Ba II	56	2.17	1.25(1)	-0.92	-0.02
La II	57	1.13	1.06±0.02(2)	-0.07	+0.83
Ce II	58	1.58	2.34±0.02(7)	+0.76	+1.66
Nd II	60	1.45	1.63(1)	+0.18	+1.08

^a Asplund et al. (2005)

Numbers within parenthesis in column 4 indicate the number of lines used for abundance estimate.

Table 9 : Elemental abundances in HD 198269

	Z	solar $\log \epsilon^a$	$\log \epsilon$	[X/H]	[X/Fe]
C	6	8.39	8.9	+0.41	+2.30
N	7	7.78	7.6 ^b	-0.18	+1.71
O	8	8.66	7.1	-1.56	+0.33
Na I	11	6.17	4.30	-1.87	+0.16
Mg I	12	7.53	6.03±0.09(3)	-1.50	+0.53
Ca I	20	6.31	4.78±0.14(8)	-1.53	+0.52
Sc II	21	3.05	1.51(1)	-1.54	+0.51
Ti I	22	4.90	3.09±0.14(7)	-1.81	+0.22
Ti II	22	4.90	3.33±0.22(13)	-1.57	+0.48
V II	23	4.00	2.1(1)	-1.9	+0.13
Cr I	24	5.64	3.53±0.18(5)	-2.11	-0.08
Mn I	25	5.39	3.23±0.16(3)	-2.16	-0.13
Fe I	26	7.45	5.42±0.17(29)	-2.03	-
Fe II	26	7.45	5.40±0.13(8)	-2.05	-
Ni I	28	6.23	4.19±0.14(5)	-2.04	-0.01
Sr I	38	2.92	1.95(1)	-0.97	+1.06
Y II	39	2.21	0.38(1)	-1.83	+0.22
Ba II	56	2.17	1.36±0.06(3)	-0.81	+1.24
La II	57	1.13	0.65±0.14(2)	-0.48	+1.57
Ce II	58	1.58	1.19±0.15(10)	-0.39	+1.66
Pr II	59	0.71	0.15±0.09(4)	-0.56	+1.49
Nd II	60	1.45	0.88±0.11(11)	-0.57	+1.48
Sm II	62	1.01	0.84±0.13(12)	-0.17	+1.88
Eu II	63	0.52	-	-	-
Er II	68	0.93	0.43(1)	-0.50	+1.55
W I	74	1.11	1.94(1)	+0.83	+2.88
Os I	76	1.45	1.07(1)	-0.38	+1.67
Pb I	82	2.00	2.5(1)	+0.5	+2.4

^a Asplund et al. (2005), ^b Vanture (1992b)

Numbers within parenthesis in column 4 indicate the number of lines used for abundance estimate.

Table 10 : Elemental abundances in HD224959

	Z	solar $\log\epsilon^a$	$\log\epsilon$	[X/H]	[X/Fe]
C	6	8.39	8.0	-0.39	+2.01
N	7	7.78	8.2 ^b	+0.42	+1.98
O	8	8.66	6.6	+2.06	+0.34
Na I	11	6.17	3.95	-2.22	+0.20
Mg I	12	7.53	5.50	-2.03	+0.39
Ca I	20	6.31	4.29±0.06(4)	-2.02	+0.40
Ti I	22	4.90	2.92±0.15(4)	-1.98	+0.44
Ti II	22	4.90	2.97±0.21(8)	-1.93	+0.49
Cr I	24	5.64	2.98±0.16(2)	-2.66	-0.24
Fe I	26	7.45	5.03±0.15(21)	-2.42	-
Fe II	26	7.45	5.03±0.23(8)	-2.42	-
Ni I	28	6.23	3.90(1)	-2.33	+0.09
Sr I	38	2.92	2.0(1)	-0.92	+1.50
Sr II	38	2.92	-	-	-
Y I	39	2.21	-	-	-
Y II	39	2.21	0.01(1)	-2.2	+0.22
Ba II	56	2.17	1.82±0.12(3)	-0.35	+2.07
La II	57	1.13	1.21±0.05(2)	+0.08	+2.50
Ce II	58	1.58	1.44±0.17(8)	-0.14	+2.28
Pr II	59	0.71	0.64±0.11(3)	-0.07	+2.35
Nd II	60	1.45	1.33±0.09(10)	-0.12	+2.30
Sm II	62	1.01	1.36±0.25(8)	+0.35	+2.07
Eu II	63	0.52	0.09(1)	-0.43	+2.01
Pb I	82	2.00	3.3(1)	+1.3	+3.70

^a Asplund et al. (2005), ^b Vanture (1992b)

Numbers within parenthesis in column 4 indicate the number of lines used for abundance estimate.

Table 11: Abundance ratios

Star	[Fe I/H]	[Fe II/H]	[Fe/H]	[Sr/Fe]	[Y/Fe]	[Zr/Fe]	[Ba/Fe]	[La/Fe]	Ref
HD 26	-1.11	-1.15	-1.13	1.89	0.89	1.16	1.93	1.53	1
	-	-	-1.25	-	-	0.9±0.3	-	2.3 ^{+0.1}	2
	-	-	-0.4	-	1.0±0.03	0.9±0.3	-	-0.5	3
	-	-	-0.3	-	-	-	-	1.4±0.4	4
			-0.45	-	-	0.6±0.41	-	2.27±0.34	5
HD 100764	-0.82	-0.90	-0.86	-	-0.08	-	-0.02	+0.83±0.02	1
HD 198269	-2.03	-2.05	-2.04	1.06	0.22	-	1.24	1.57±0.14	1
	-	-	-2.2±0.2	-	-	0.4±0.1	-	1.6±0.2	2
	-	-	-1.4	-	-	1.2±0.1	-	1.4±0.4	3
HD 224959	-2.42	-2.42	-2.42	1.50	0.22	-	2.07±0.12	2.50±0.08	1
	-	-	-2.2±0.2	-	-	1.0±0.1	-	2.3±0.2	2
	-	-	-1.6	-	-	-	-	2.0±0.6	3

1.This work, 2. Van Eck et al. (2003), 3. Vanture (1992c), 4. Thevenin and Idiart (1999), 5. Luck and Bond (1982)

Table 11: Abundance ratios (Continued)

Star	[Ce/Fe]	[Pr/Fe]	[Nd/Fe]	[Sm/Fe]	[Eu/Fe]	[Er/Fe]	[W/Fe]	[Os/Fe]	[Pb/Fe]	Ref
HD 26	1.65±0.13	1.64±0.17	1.45±0.10	1.88±0.30	0.68	1.44	3.54	-	2.55±0.30	1
	1.7 ^{+0.3}	-	1.3 ^{+0.3}	1.3±0.3	-	-	-	-	2.0±0.2	2
	-0.4	-	-0.1	1.9±0.2	-	-	-	-	-	3
	1.9±0.4	-	1.6±0.15	1.99	0.40	-	-	-	-	5
HD 100764	1.66±0.02	-	1.08	-	-	-	-	-	-	1
HD 198269	1.66±0.15	1.49±0.09	1.48±0.11	1.88±0.13	-	1.55	2.88	1.67	2.4	1
	1.5±0.3	-	1.2±0.1	1.2±0.2	-	-	-	-	2.4±0.2	2
	1.6±0.3	-	1.0±0.2	0.9±0.2	-	-	-	-	-	3
HD 224959	2.28±0.17	2.35±0.11	2.30±0.09	2.07±0.25	2.01	-	-	-	2.7	1
	1.9±0.3	-	2.0±0.2	1.9±0.2	-	-	-	-	3.1±0.2	2
	2.1±0.1	-	1.8±0.3	1.4±0.15	-	-	-	-	-	3

1. This work, 2. Van Eck et al. (2003), 3. Vanture (1992c), 5. Luck and Bond (1982)

Table 12 : Component coefficients and reduced χ^2_ν from parametric model based analysis

Objects	[Fe/H]	A_s	A_r	χ^2_ν
HD 26	-1.13	0.69±0.09	0.31±0.08	3.2
HD 198269	-2.04	0.07±0.06	0.88±0.06	4.1
HD 224959	-2.42	-0.03±0.08	0.98±0.07	5.4

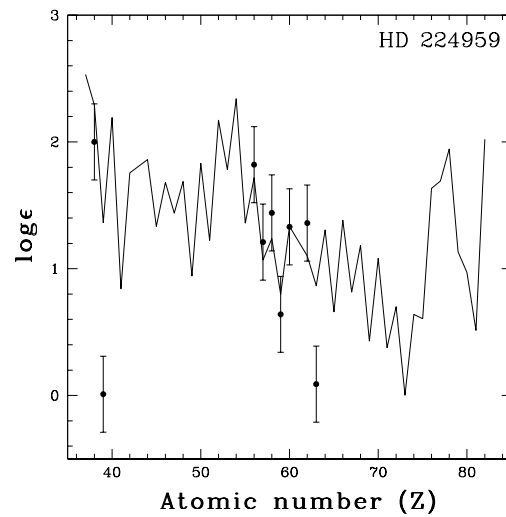
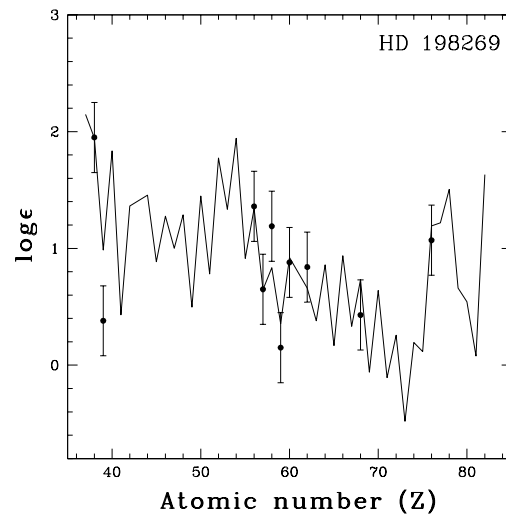
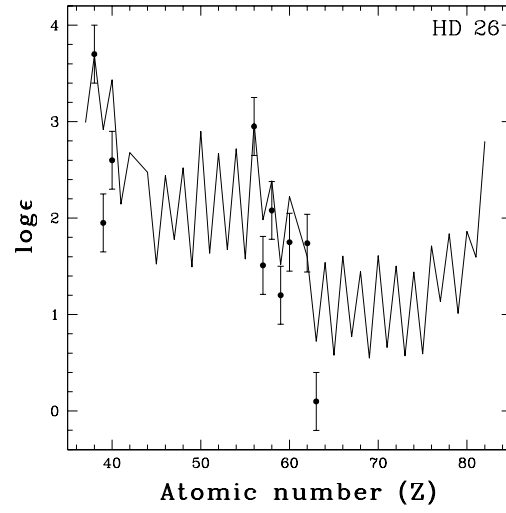


Figure 7. Solid curves represent the best fit for the parametric model function $\log \epsilon = A_s N_{si} + A_r N_{ri}$, where N_{si} and N_{ri} represent the abundances due to s- and r-process respectively (Arlandini et al. 1999, Stellar model, scaled to the metallicity of the star). The best fit coefficients A_s , A_r and their respective reduced chisquare are listed in Table 11. The points with errorbars indicate the observed abundances.

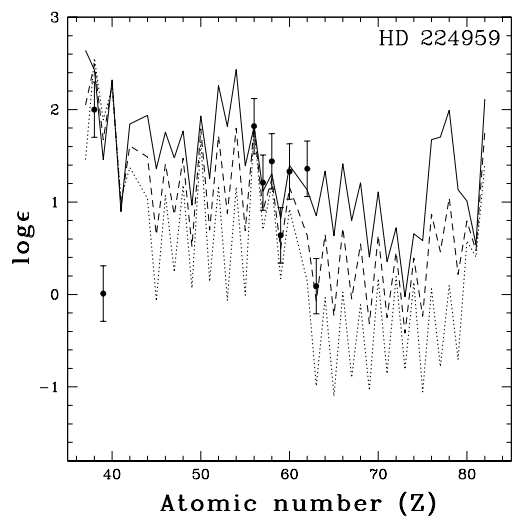
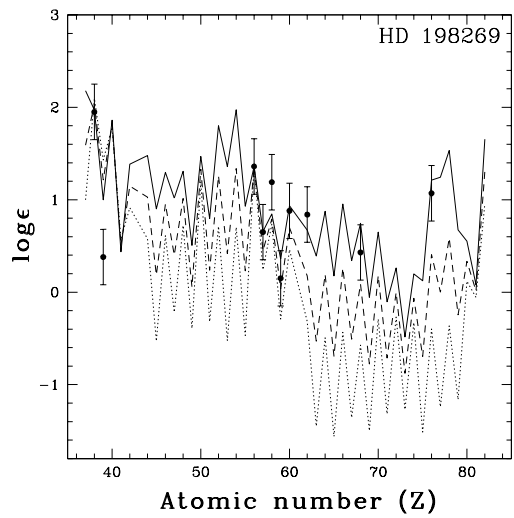
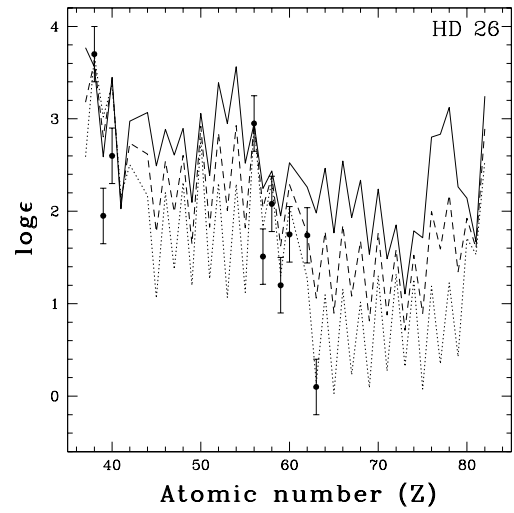


Figure 8. Abundance patterns of heavy elements from Arlandini et al. (1999) (Stellar model). Solid line shows abundances due to only r-process; dotted line is of s-process only and dashed line indicates abundance pattern derived from a simple average of r- and s-processes. The abundances are scaled to the metallicity of the star and normalized to the observed Ba abundances. The points with errorbars indicate the observed abundances.

Calculated coefficients indicate dominance of r-process on abundances of the heavy elements in case of HD 198269 and HD 224959 and the dominance of s-process in case of HD 26. It is noticed in Figure 8, that the abundance pattern of elements $56 \leq Z \leq 63$ in HD 26 agree with the s-process pattern much better than with the r-process.

8 DISCUSSION AND CONCLUDING REMARKS

Results from abundance analysis for three early type CH stars and a carbon star with a cool dusty envelope listed in the CH star catalogue (Bartkevicius 1996) are presented. The earlier chemical abundance studies of these objects were limited to few elements and carbon isotopic ratios and also limited by both spectral resolution and wavelength region. We have conducted a detailed chemical composition study of these objects using high-resolution Subaru spectra covering a wavelength region from 4020 to 6775 Å. We could achieve better accuracy in abundance estimates with a much lower error range 0.1 - 0.3 dex compared to those reported previously (i.e. Vanture 1992c). New abundance estimates for several neutron-capture elements such as Sr, Y, Zr, Ba, La, Sm, Eu, Er, W, and Pb are presented. All the stars display larger enhancement of the 2nd-peak s-process elements such as Ba, La, Ce, Nd, Sm etc. compared to the 1st-peak s-process elements Sr, Y, and Zr. Compared to Sun ($[\text{Sr}/\text{Ba}] = 0.74$), these stars show a much smaller ratio of $[\text{Sr}/\text{Ba}]$, i.e. -0.04 (HD 26), -0.18 (HD 198269), and -0.57 (HD 224959). In case of HD 100764 we could measure abundances for only four heavy elements Y, La, Ce and Nd; and the abundance ratios with $[\text{Y}/\text{Fe}] = -0.08$, $[\text{La}/\text{Fe}] = 0.83$, $[\text{Ce}/\text{Fe}] = 1.66$ and $[\text{Nd}/\text{Fe}] = 1.08$ are smaller compared to solar ratios. Abundance of Zn measured from a single Zn I line gives a near-solar value for this object. While the abundances of Ba could be estimated for all the four objects, the abundance estimate for Eu was possible only for HD 26 and HD 224959 using our spectra. For HD 224959 our estimated $[\text{Ba}/\text{Eu}] = 0.06$, but HD 26 shows a high value with $[\text{Ba}/\text{Eu}] \sim 1.32$.

Taking into consideration the range of $[\text{Ba}/\text{Fe}]$, $[\text{Eu}/\text{Fe}]$ and $[\text{Ba}/\text{Eu}]$ (Beers & Christlieb 2005, Masseron et al. 2010, Jonsell et al. 2006) for distinguishing CEMP-s stars from CEMP-r/s stars, we find that none of our program stars qualify to be a CEMP-r/s star. At the non-availability of Eu abundance, CEMP stars with $[\text{Ba}/\text{Fe}] \geq 2.1$ are classified as CEMP-r/s star (Masseron et al. 2010). None of our objects show enhancement of Ba abundance as high as this value. HD 224959 with $[\text{Ba}/\text{Fe}] = 2.07$ is found to marginally meets this criterion. HD 198269 with $[\text{Ba}/\text{Fe}] = 1.24$ also does not qualify to be a CEMP-r/s star, and same is the case for HD 26 with $[\text{Ba}/\text{Fe}] = 1.93$, $[\text{Eu}/\text{Fe}] = 0.61$ and $[\text{Ba}/\text{Eu}] > 1.32$. In the case of HD 224959 the estimated $[\text{Eu}/\text{Fe}] = 2.01$ satisfies the condition for CEMP-r star (CEMP-r: $[\text{C}/\text{Fe}] > 1.0$ and $[\text{Eu}/\text{Fe}] > +1.0$); whereas with $[\text{Ba}/\text{Eu}] = 0.06$ this object also satisfies the condition for CEMP-r/s star (CEMP-r/s: $[\text{C}/\text{Fe}] > 1.0$ and $0 < [\text{Ba}/\text{Fe}] < 0.5$). As none of the previous authors reported on Eu abundance for these objects, a direct comparison of Eu abundances estimated for HD 224959 and HD 26 was not possible.

There are a lot of ambiguities in the classification of lead stars, as well as CEMP stars, in particular distinguishing between CEMP-s and CEMP-r/s stars. For a well founded classification of these objects more tighter relations are needed. The estimates of abundance ratios of neutron-capture elements observed in the present sample (Table 11), if extended for a larger sample of CH stars covering a wide range in metallicity, will allow to set a limit on metallicity of stars showing enhanced abundances of s-process and/or both s- and r-process elements.

Except for HD 100764, we have estimated the abundance of lead, the 3rd-peak s-process element, for the other three stars in

our sample. Pb shows large enhancements with $[\text{Pb}/\text{Fe}] = 2.11$ (HD 26), 2.4 (HD 198269) and 3.7 (HD 224959). Enhancement of Pb abundance is noticed in a number of CH as well as CEMP-(r+s) stars. Van Eck et al. (2003) defined stars with $[\text{Pb}/\text{hs}] \geq +1.0$ as ‘lead stars’, where hs includes Ba, La and Ce. According to Jonsell et al. (2006) ‘lead stars’ are those with $[\text{Pb}/\text{Ba}] \geq 1.0$. This definition does not require the ‘lead stars’ also to be (r+s) stars, but requires that they are enhanced in Ba and Pb, and much more in the latter element. Estimated $[\text{Pb}/\text{Ba}]$ in HD 26, 198269 and 224959 are respectively 0.74, 1.14 and 0.69. Following the definition of Jonsell et al. 2006 the star HD 198269 satisfies the criteria to be a lead star. LP 625–44 and LP 706–7, both enriched in s-process elements including Pb, were not considered as ‘lead stars’ by Aoki et al. (2001) as they show low values of $[\text{Pb}/\text{Ce}] \leq 0.4$; alternatively, they suggest, $[\text{Pb}/\text{Ce}] \geq 0.4$ could be a criterion for classifying a star as a ‘lead star’. This requirement in the abundance ratio of $[\text{Pb}/\text{Ce}]$ is met by all the three stars studied here with $[\text{Pb}/\text{Ce}] = 0.46$ (HD 26), 0.74 (HD 198269), 1.42 (HD 224959).

Models of very low-metallicity AGB stars developed in the framework of the partial mixing of protons into the deep carbon-rich layers predict overabundance of Pb-Bi as compared to lighter s-elements. These stars are characterized by large $[\text{Pb}/\text{Fe}]$, $[\text{s}/\text{Fe}]$ and $[\text{Pb}/\text{s}]$ abundance ratios. In this scenario, AGB stars with $[\text{Fe}/\text{H}] \geq -1.3$, are predicted to exhibit $[\text{Pb}/\text{hs}]$ (where hs refers to heavy s-process elements, such as Ba, La or Ce) ratios as large as 1.5. These model predictions are robust with respect to the model parameters, i.e., the abundance profile of the protons in the partially mixed layers or the extent of the partial mixing zone and uncertainties in the reaction rates (Van Eck et al. 2001). In agreement with the model predictions the three CH stars under this study are found to exhibit overabundance of Pb with respect to other s-process elements. High spectral resolution is essential to resolve the 4057.81 Å Pb I line from the nearby CH line at 4057.7 Å and therefore to derive correct lead abundances. We note that our spectra do not have very good signal at this spectral region. Other Pb I lines at 4063 Å are not detectable in our spectra and Pb I 7228.97 Å line is out of our wavelength region.

Some of the previous reports (Snedden et al. 1998, 2000; Aoki et al. 2000) with large lead overabundances in low-metallicity stars are found not to satisfy all these conditions. In these studies, the overabundances of lead are attributed to the r-process rather than the s-process, because they occur with strong enhancement of the r-process element Eu. For instance, LP 625-44 shows $[\text{Pb}/\text{Fe}] = 2.65$, but $[\text{Pb}/\text{La}] = 0.15$ and $[\text{Pb}/\text{Ba}] = -0.09$ (Aoki et al. 2000). Our estimated $[\text{Pb}/\text{La}]$, $[\text{Pb}/\text{Ba}]$, $[\text{Pb}/\text{Ce}]$, $[\text{Pb}/\text{Sm}]$ and $[\text{Pb}/\text{Nd}]$ values are respectively (0.58, 0.18, 0.46, 0.23, 0.66) for HD 26, (0.83, 1.16, 0.74, 0.52, 0.92) for HD 198269 and (1.2, 1.63, 1.42, 1.63, 1.4) for HD 224959. Usually, $[\text{Pb}/\text{H}]$ is expected to decrease with increasing metallicity from $[\text{Fe}/\text{H}] = -2$ to -1 (Käppeler et al. 2011); our results are in agreement with this.

We have compared the derived abundances (scaled to Ba abundance) with the predicted elemental abundances at the surface of AGB stars at four different metallicities ($z = 0.018$, $z = 0.08$, $z = 0.004$ and $z = 0.001$) in the dredge-up material, 10th, 30th and 50th pulses of Goriely and Mowlavi (2000). In this scenario the primary ^{13}C pocket formed in the proton-mixing zone at low proton-to- ^{12}C ratios is found to be responsible for an efficient production of s-process nuclei. None of the model predictions show a proper match with the observed abundances.

In Figure 8, we have compared the resulting abundances of neutron-capture elements for HD 26, 198269 and 224959 along with the scaled abundance patterns of the solar system material, the main s-process component, and the r-process pattern (Arlan-dini et al. 1999). The abundance patterns of elements with $56 \leq Z \leq 63$ agree with the s-process pattern much better than with the r-process pattern indicating that the neutron-capture elements in

HD 26 principally originate in the s-process. Estimated $[\text{Ba}/\text{Eu}]$ ($= 1.32$) for HD 26 is similar to that seen in the main s-process component ($[\text{Ba}/\text{Eu}] = 1.15$, Arlandini et al. 1999), but much lower in the case of HD 224959 with $[\text{Ba}/\text{Eu}] = 0.06$. The abundance patterns of elements $56 \leq Z \leq 63$ are however in agreement with the s-process pattern. The observed low values of $[\text{Ba}/\text{Eu}]$ in HD 224959 may be interpreted as a result of an s-process that produces different abundance ratios from that of the main s-process component (Aoki et al. 2002). This idea needs further investigation.

Theoretical models of Goriely & Mowlavi (2000) predicted $[\text{Ba}/\text{Eu}] = 0.4$ for yields of metal-deficient AGB stars. Analyses of the observed abundances of the heavy elements for HD 26 based on a parametric model show that s-process have higher contributions with $A_s \sim 0.69$ than r-process with $A_r \sim 0.31$, where A_s and A_r are the component coefficients that correspond to contributions from the s- and r-process respectively. Here, the contributions from r- and s-process are estimated from the fitting for Ba - Er.

High velocities are a common feature of CH stars. Temporal variations of radial velocities observed among the known CH stars indicate binarity of the objects. This is in support of the widely accepted scenario for the formation of CH stars, involving mass transfer from a companion AGB star (McClure 1983, 1984 and McClure and Woodsworth 1990). While the radial velocity estimate for HD 100764 is $\sim 5 \text{ km s}^{-1}$, the other three objects are high-velocity stars (Table 2). The high radial velocities suggest halo membership. Our estimates of radial velocities compare well with literature estimates that confirmed these objects to be radial velocity variables (McClure and Woodsworth 1990) with periods of 3.55 yrs (HD 198269) and 3.49 yrs (HD 224959). Kinematic properties support a physical scenario in which the observed enhancement of neutron-capture elements resulted from a transfer of material rich in s-process elements across a binary system with an AGB star.

Acknowledgment

This work made use of the SIMBAD astronomical database, operated at CDS, Strasbourg, France, and the NASA ADS, USA. Funding from the DST project SB/S2/HEP-010/2013 is gratefully acknowledged.

REFERENCES

- Abate C., Pols, O. R.; Izzard, R. G.; Mohamed, S. S.; de Mink, S. E., 2013, A&A, 552, 26
- Alonso A., Arribas S. & Martinez-Roger C., 1994 A&AS, 107, 365
- Alonso A., Arribas S. & Martinez-Roger C., 1996 A&A, 313, 873
- Andersen T., Poulsen, O., Ramanujam, and Petrakiev Petkov, A. 1975, Solar Phys 44, 257-267.
- Arribas S., Martinez-Roger C., 1987, A&AS, 70, 303
- Arnesen A., Bengtsson A., Hallin R., Lindsog J., Nordling C., and Noreland T. 1977, Phys.Scripta 16, 31-34.
- Aoki W., Norris J. E., Ryan S. G., Beers, T. C., & Ando, H. 2000, ApJ, 536, L97
- Aoki W. & Tsuji T., 1997, A&A, 317, 845
- Aoki W., Ryan S. G., Norris J. E., et al., 2001, ApJ, 561, 346
- Aoki W., Ryan S. G., Norris J. E., Beers T. C., Ando H., & Tsangarides S., 2002, ApJ, 580, 1149
- Aoki W. et al., 2005, ApJ, 632, 611
- Aoki W., Beers T.C., Christlieb N., Norris J.E., Ryan S.G., & Tsangarides S., 2007, ApJ, 655, 492
- Arlandini, C., Käppeler, F., Wisshak, K. et al., 1999, ApJ, 525, 886
- Asplund M., Grevesse N. & Sauval A. J., 2005, ASPC, 336, 25
- Asplund M., Grevesse N. & Sauval A. J., Scott P., 2009, ARA&A, 47, 481
- Bartkevicius, A., 1996, BaltA, 5, 217
- Baumüller D., Gehren T., 1997, A&A, 325, 1088
- Baumüller D., Butler K., Gehren T., 1998, A&A, 338, 637
- Barbuy, B., Spite, M., Spite, F., Hill, V., Cayrel, R., Plez, B., Petitjean, P., 2005, A&A, 429, 1031
- Beers T. C. & Christlieb N., 2005, ARA&A, 43, 561
- Bergeat J., Knapik A., Rutily, B., 2001, A&A, 369, 178
- Biemont E., Grevesse N., Hannaford p., Lowe R. M., 1981, ApJ, 248, 867
- Biemont E., Karner C., Meyer G., Traeger F., and zu Putlitz G. 1982, A&A 107, 166-171.
- Cayrel, R., Depagne, E., Spite. M., Hill, V., Spite, F., Francois, P., Plez, B., Beers, T. C., et al., 2004, A&A, 416, 1117
- Christlieb N., 2003, RvMA, 16, 191
- Corliss C.H. and Bozman W.R. 1962, NBS Monograph 53.
- Corliss C.H. and Bozman W.R. 1962, NBS Monograph 53. adjusted
- Cutri R. M. et al., 2003, Explanatory Supplement to the 2MASS All Sky Data Release, <http://www.ipac.caltech.edu/2mass/releases/allsky/doc/explsups.html>
- Dominy, J. F. 1984, ApJS, 55, 27
- El Eid, M. F., & Champagne, Arthur E., 1995, ApJ, 451, 298
- Fuhr J. R., Martin G. A., Wiese W. L., 1988, J. Phys. Chem. Ref. Data, 17, 4
- Goriely S., Mowlavi N., 2000, A&A, 362, 599
- Goswami A., Prantzos N., 2000, A&A, 359, 191
- Goswami A., Aoki W., Beers T.C., Christlieb N., Norris J. E., Ryan S. G., Tsangarides T., 2006, MNRAS, 372, 343
- Goswami A., & Aoki W., 2010, MNRAS, 404, 253
- Hannaford P., Lowe R.M., Grevesse N., Biemont E., and Whaling W 1982, ApJ 261, 736-746.
- Hartwick, F. D. A. & Cowley, A. P., 1985, AJ, 90, 224
- Hollowell, David; Iben, Icko, Jr., 1988, ApJ, 333, 25
- Howard, W. M., Mathews, G. J., Takahashi K., Ward, R. A., 1986, ApJ, 309, 633
- Jonsell K., Barklem P. S., Gustafsson B., Christlieb N., Hill V., Beers T. C., Holmberg J., 2006, A&A, 451, 651
- Käppeler, F., Gallino, R., Bisterzo, S., Aoki, W., 2011, RvMP, 83, 157
- Karinkuzhi, D & Goswami, A, 2014, MNRAS, 440, 1095
- Karinkuzhi, D & Goswami, A, 2015, MNRAS, 446, 2348
- Keenan, Philip C., 1942, ApJ, 96, 101
- Keenan, Philip C., 1993, PASP, 105, 905
- Lambert D. L., Heath J. E., Lemke M., Drake J., 1996, ApJS, 103, 183
- Lage C.S. and Whaling W. 1976, JQSRT 16, 537-542.
- Lawler J. E., Bonvallet G., Sneden C., 2001, ApJ, 556, 452
- Lee P., 1974, ApJ, 192, 133
- Lucatello S., Gratton R., Cohen J. G., et al. 2003, AJ, 125, 875
- Lucatello S., Gratton R. G., Beers T. C., Carretta E., 2005, ApJ, 625, L833
- Luck R. E. & Bond H. E., 1982, ApJ, 259, 792
- McClure R. D., 1983, ApJ, 268, 264
- McClure R. D., 1984, ApJ, 280, L31
- McClure R. D., Woodsworth W., 1990, ApJ, 352, 709
- McEachran R.P., and Cohen M. 1971, JQSRT, 11, 1819.
- Meggers W.F., Corliss C.H. and Scribner B.F. 1975, NBS Monograph 145. estimated from intensity
- Martin G. A., Fuhr J. R., Wiess, W. L., 1988, J. Phys. Chem. Ref. data, 17, 3
- Masseron, T., Johnson, J. A., Plez, B., Van Eck, S., Primas, F., Goriely, S., Jorissen, A., 2010, A&A, 509, A93
- McWilliam A., Preston G. W., Sneden C., Searle L., 1995a, AJ, 109, 2736
- McWilliam A., Preston G. W., Sneden C., Searle L., 1995b, AJ, 109, 2757
- McWilliam A., 1998, AJ, 115, 1640

Meggers, W.F, Corliss, C.H. and Scribner, B.F. 1975, NBS Monograph 145

Miles, B.M. and Wiese, W.L. 1969, NBS Technical Note 474

Noguchi K. et al., 2002, PASJ, 54, 855

Nordstroem, B., Mayor, M., Andersen, J., Holmberg, J., Pont, F., Jorgensen B.R., Olsen E.H., Udry S., Mowlavi N., 2004, A&A, 418, 989

Norris J. E., Ryan S.G., Beers, T. C. 1997a, ApJ, 488, 350

Norris J. E., Ryan S.G., Beers T. C. 1997b, ApJ, 489, L169

Norris J. E., Ryan S.G., Beers T. C., Aoki, W & Ando H., 2002, ApJ, 569, L107

Obbarius, H.U. and Kock, M. 1982, J. Phys. B 15, 527-534

Phillips, J. G. and Davis, S. P. 1968, ZA, 69, 385

Platais I. et al., 2003, A&A, 397, 997

Prantzos, N., Arnould M., Arcoragi, JP., 1987, ApJ, 315, 209

Prochaska, J. X., & McWilliam A., 2000, ApJ, 537, L57

Roederer, I. U., Frebel, A., Shetrone, M. D., et al. 2008, ApJ, 679, 1549

Ryan S. G., Norris J. E., Beers T. C., 1996, ApJ, 471, 254

Saffman L. and Whaling W. 1979, JQSRT 21, 93-98.

Salih, S. and Lawler, J.E. 1985, JOSA B 2, 422-425.

Smith V V, & Lambert, D. L., 1986, ApJ, 303, 226

Sneden C., 1973, PhD thesis, Univ of Texas at Austin

Sneden C., Cowan J. J., Burris D. L., Truran J. W., 1998, Apj, 496, 235

Sneden C., Johnson J., Kraft R. P., Smith G. H., Cowan J. J., Bolte M. S., 2000, ApJ, 563L, 85

Sneden C., McWilliam A., Preston G.W.,Cowan J. J., Burris D. L., Armosky B. J., 1996, ApJ, 467, 819

Thevenin, F. & Idiart, T. P., 1999, ApJ, 521, 753

Truran, J. W., 1981, A&A, 97, 391

Van Eck, S., Goriely, S., Jorissen, A., Plez, B. 2001, Nature, 412, 793

Van Eck S., Goriely S., Jorissen, A., Plez, B. 2003, A&A, 404, 291

Vanture A. D., 1992a, AJ, 103, 2035

Vanture A. D., 1992b, AJ, 104, 1986

Vanture A. D., 1992c, AJ, 104, 1997

Ward L., Vogel O., Arnesen A., Hallin R., and Wannstrom A. 1985, Phys. Scripta 31, 162-165.

Wiese W.L., Smith M.W., and Glennon B.M. 1966, NSRDS-NBS 4.

Wheeler J. Craig, Sneden C., Truran James W. Jr., 1989, ARAA, 27, 279

Wolnik S.J. and Berthel R.O. 1973, ApJ 179, 665

Zijlstra A. A., 2004, MNRAS, 348, L23

Table 13: Equivalent widths

Wlab	id	Z	Elow	log gf	HD 26	HD 100764	HD 198269	HD 224959	Ref
5889.95	Na I	11.0	0.00	0.10	324.3	-	258.5	184.9	1
5895.92		11.0	0.00	-0.20	284.3	-	240.4	175.6	1
4057.50	Mg I	12.0	4.35	-0.89	-	-	98.35	-	2
4571.10		12.0	0.00	-5.69	-	-	151.9	57.76	2
5172.69:		12.0	2.71	-0.38	-	-	324.7	185.8	2
5528.40		12.0	4.35	-0.34	184.6	-	151.0	122.6	3
5588.76	Ca I	20.0	2.53	0.36	-	-	121.0	57.3	3
5594.47		20.0	2.52	0.10	-	-	118.8	-	3
5598.49		20.0	2.52	-0.09	-	-	116.9	-	3
5857.45		20.0	2.93	0.24	-	-	95.19	-	3
6102.72		20.0	1.88	-0.77	117.2	-	110.0	41.7	3
6122.22		20.0	1.89	-0.32	151.4	-	143.8	-	3
6162.17		20.0	1.90	-0.09	-	-	164.4	93.6	3
6439.07		20.0	2.53	0.39	144.4	-	137.0	73.4	3
6462.567:		20.0	2.52	0.26	-	-	-	182.2	3
4415.54	Sc II	21.1	0.60	-0.89	-	-	88.56	-	3
5031.01		21.1	1.36	-0.40	-	-	107.6	-	3
# 6245.630		21.1	1.51	-1.03	hfs-syn	-	hfs-syn	hfs-syn	3
4533.239	Ti I	22.0	0.85	0.48	113.0	-	105.7	54.2	4
4534.778		22.0	0.84	0.28	108.1	-	105.6	60.2	4
4981.73		22.0	0.85	0.50	-	-	124.7	-	4
4991.067		22.0	0.84	0.38	-	-	126.4	57.6	4
5039.96		22.0	0.02	-1.13	-	-	107.8	-	4
5064.65		22.0	0.05	-0.99	-	-	115.2	-	4
5210.386		22.0	0.05	-0.88	-	-	117.6	49.2	4
4025.12:	Ti II	22.1	0.61	-1.98	-	-	119.9	-	4
4053.83:		22.1	1.89	-1.21	-	-	67.69	-	4
4287.88:		22.1	1.08	-2.02	-	-	122.3	52.4	4
4344.30:		22.1	1.08	-2.09	-	-	126.0	-	4
4418.31		22.1	1.24	-1.99	120.0	-	72.43	-	4
4443.77		22.1	1.08	-0.70	163.0	-	168.4	113.7	4
4450.50		22.1	1.08	-1.51	-	-	135.5	79.9	3
4464.46:		22.1	1.16	-2.08	-	-	116.1	-	4
4501.27		22.1	1.12	-0.76	-	-	164.7	122.5	4
4529.48:		22.1	1.57	-2.03	-	-	101.7	-	4
4563.77		22.1	1.22	-0.96	173.1	-	160.2	119.4	4
4571.96		22.1	1.57	-0.53	-	-	187.1	-	4
4589.92:		22.1	1.24	-1.79	-	-	107.1	57.0	4
4657.21		22.1	1.24	-2.32	-	-	74.6	-	4
4779.98		22.1	2.05	-1.37	-	-	74.0	-	4
4798.51		22.1	1.08	-2.67	-	-	86.2	-	3
4805.09		22.1	2.06	-1.10	-	-	105.4	68.4	4
4865.61		22.1	1.12	-2.81	77.1	-	65.3	-	4
5185.90		22.1	1.89	-1.35	-	-	87.0	38.3	4
5226.53		22.1	1.57	-1.30	-	-	122.9	-	4
# 5727.048	V I	23.1	1.08	-0.012	hfs-syn	-	hfs-syn	hfs-syn	3
4254.33	Cr I	24.0	0.00	-0.11	-	-	183.9	-	4
4600.75		24.0	1.00	-1.26	-	-	79.4	-	4
4616.12		24.0	0.98	-1.19	-	-	99.0	-	4
4626.19		24.0	0.97	-1.32	88.2	-	-	-	4
4646.17		24.0	1.03	-0.70	-	-	102.9	41.8	4
4652.16		24.0	1.00	-1.03	-	-	107.0	-	4
5206.04		24.0	0.94	0.02	-	-	162.4	78.7	4
4451.58:	Mn I	25.0	2.89	0.28	-	-	118.0	-	4
4754.05		25.0	2.28	-0.09	-	-	77.3	-	4
4783.43		25.0	2.30	0.04	-	-	100.7	-	4
4823.53		25.0	2.32	0.14	-	-	106.5	-	4
# 6013.488		25.0	3.072	-0.250	syn	syn	syn	syn	4

Table 13: Equivalent widths (continued)

Wlab	id	Z	Elow	log gf	HD 26	HD 100764	HD 198269	HD 224959	Ref
4855.41	Ni I	28.0	3.54	0.00	-	-	51.8	18.6	5
4980.16		28.0	3.61	-0.11	89.5	-	53.8	-	5
5035.37		28.0	3.63	0.29	79.2	-	60.4	-	5
5080.52		28.0	3.65	0.13	-	-	65.0	-	5
5137.08		28.0	1.68	-1.99	-	-	93.0	-	5
4810.53		30.0	4.08	-0.17	84.2	-	-	-	3
4607.327	Sr I	38.0	0.00	-0.57	syn	syn	syn	syn	6
6550.24:		38.0	2.69	+0.18	-	104.8	42.6	-	6
4883.685	Y II	39.1	1.08	0.07	149.4	101.0	113.9	-	7
5087.43		39.1	1.08	-0.17	-	229.9	-	-	7
5200.413		39.1	0.99	-0.57	syn	syn	syn	syn	7
5205.73		39.1	1.03	-0.34	-	-	86.2	45.3	7
5473.388:		39.1	1.74	-1.02	-	-	23.6	-	7
4414.124:	Zr I	40.0	0.15	-2.32	-	56.09	67.2	-	6
5311.434:		40.0	0.52	-1.71	-	-	54.3	-	6
6134.585:		40.0	0.00	-1.28	syn	-	syn	syn	8
4443.00:	Zr II	40.1	1.49	-0.33	-	-	254.3	-	8
4496.97:		40.1	0.71	-0.59	-	-	20.6	-	8
4812.281	Mo I	42.0	3.26	-1.90	-	-	34.4	-	9
5204.552		42.0	3.36	-1.87	-	253.5	37.2	100.8	9
5298.010		42.0	2.68	-1.85	-	-	207.3	-	9
5991.370		42.0	3.44	-1.64	-	73.7	25.7	-	9
5752.022	Rb I	44.0	1.00	-2.96	-	-	18.2	-	10
4554.036	Ba II	56.1	0.00	0.12	-	250.7	-	-	2
4934.076		56.1	0.00	-0.15	-	292.7	356.5	332.1	1
# 5853.668		56.1	0.60	-1.02	hfs-syn	153.2	hfs-syn	hfs-syn	1
6141.727		56.1	0.70	-0.08	syn	syn	250.8	245.5	1
6496.897		56.1	0.60	-0.38	-	235.7	252.1	-	1
4086.709	La II	57.1	0.00	-0.15	-	116.2	-	-	11
4322.51:		57.1	0.17	-1.05	-	-	102.1	97.4	12
4526.111:		57.1	0.77	-0.77	81.9	46.4	57.7	-	11
4580.045		57.1	0.71	-1.02	-	-	-	51.5	12
4662.51:		57.1	0.00	-1.28	99.0	-	93.2	-	12
4748.726		57.1	0.93	-0.86	71.2	-	48.7	51.3	12
4840.00:		57.1	0.32	-2.07	-	9.5	44.2	44.8	12
# 4921.776			0.24	-0.68	hfs-syn	-	hfs-syn	hfs-syn	12
4999.461		57.1	0.40	-0.89	-	144.2	-	-	12
5259.38:		57.1	0.17	-1.76	-	-	43.9	-	12
6320.43:		57.1	0.17	-1.52	-	-	74.0	-	13
5328.085:	Ce I	58.0	0.49	0.01	-	-	225.7	-	14
6093.193		58.0	0.80	-0.37	-	108.1	-	-	14
6335.340		58.0	0.47	-1.32	-	133.6	-	-	14
4062.22	Ce II	58.1	1.37	0.26	-	-	41.9	36.0	14
4076.24		58.1	0.81	-0.42	-	-	43.7	-	14
4117.29		58.1	0.74	-0.525	-	-	42.4	36.0	14
4127.38:		58.1	0.68	+0.11	-	-	69.4	53.1	14
4185.33:		58.1	0.42	-0.64	-	-	48.7	-	14
4190.63		58.1	0.90	-0.47	-	-	180.8	-	14
4222.60:		58.1	0.12	-0.30	-	-	97.7	80.2	14
4257.12		58.1	0.46	-1.12	-	-	49.6	-	14
4336.244		58.1	0.70	-0.56	84.4	-	62.7	-	14
4423.673		58.1	1.06	-0.32	-	-	54.3	46.6	14
4427.92		58.1	0.54	-0.46	-	-	84.9	-	14
4486.91:		58.1	0.30	-0.36	-	14.4	96.0	77.1	14
4515.86:		58.1	1.06	-0.52	56.3	-	42.2	41.1	14
4522.079		58.1	0.87	-1.49	-	28.6	35.9	-	14
4523.075		58.1	0.51	-0.30	-	-	116.3	-	14
4527.348		58.1	0.32	-0.46	-	142.6	-	-	14
4539.745		58.1	0.32	-0.45	-	-	96.8	73.5	14
4544.96		58.1	0.42	-0.97	-	-	94.9	-	14
4551.291:		58.1	0.74	-0.58	-	116	78.6	-	14

Table 13 : Equivalent widths (continued)

Wlab	id	Z	Elow	log gf	HD 26	HD 100764	HD 198269	HD 224959	Ref
4562.37		58.1	0.48	+0.33	120.1	72.0	-	99.7	3
4628.16		58.1	0.52	+0.26	-	-	108.0	-	14
4744.944		58.1	0.44	-1.67	-	-	47.1	-	14
4747.167		58.1	0.32	-1.24	-	-	56.0	-	14
4757.841:		58.1	0.95	-0.78	-	-	43.9	-	14
4773.941		58.1	0.92	-0.49	-	-	51.4	38.9	14
4873.999:		58.1	1.10	-0.89	-	50.7	44.9	28.4	14
5022.867:		58.1	1.04	-0.72	89.7	117.4	81.8	37.8	14
5187.457:		58.1	1.21	-0.10	-	40.15	73.0	49.6	14
5274.230		58.1	1.04	0.32	92.1	94.5	71.3	59.2	14
5330.556:		58.1	0.86	-0.76	76.7	23.89	55.9	38.3	14
5512.064		58.1	1.00	-0.51	-	-	53.5	34.1	14
5975.818:		58.1	1.32	-0.81	-	-	31.1	18.3	14
5996.060	Pr I	59.0	1.20	-0.17	-	37.7	-	-	15
4148.44	Pr II	59.1	0.22	-0.72	-	-	81.1	-	15
5188.217		59.1	0.92	-1.14	-	-	24.2	-	15
5219.045		59.1	0.79	-0.24	-	-	34.4	-	16
5220.12		59.1	0.80	+0.17	-	-	58.5	58.2	3
5259.74		59.1	0.63	-0.07	86.0	-	57.8	55.9	16
5292.619		59.1	0.64	-0.30	69.4	52.5	32.6	30.6	16
5322.772:		59.1	0.48	-0.31	94.9	-	63.8	62.1	15
5331.460		59.1	0.64	-1.97	26.5	60.8	-	-	5
4051.141	Nd II	60.1	0.38	0.09	-	-	103.3	-	17
4059.951		60.1	0.20	-0.36	-	-	70.1	-	17
4061.08:		60.1	0.47	0.55	130.7	-	115.8	-	15
4069.27:		60.1	0.06	-0.40	101.6	-	92.2	-	17
4109.46		60.1	0.32	+0.28	-	-	184.2	-	15
4133.36		60.1	0.32	-0.34	-	-	102.9	-	17
4232.38:		60.1	0.06	-0.35	-	-	115.5	91.5	18
4256.821		60.1	0.18	-1.39	-	-	44.0	38.4	17
4412.256		60.1	0.06	-1.42	-	-	89.3	-	15
4446.39		60.1	0.20	-0.63	-	-	102.3	-	15
4451.563:		60.1	0.38	-0.04	134.3	131.5	118.0	108.0	20
4451.98:		60.1	0.00	-1.34	-	63.3	89.2	71.8	15
4462.979		60.1	0.55	0.07	-	-	125.2	-	15
4594.445		60.1	0.20	-1.55	64.7	-	44.7	36.4	15
4749.560		60.1	0.55	-1.55	77.7	-	34.8	-	15
4797.153		60.1	0.55	-0.95	-	-	49.2	46.5	15
4819.64:		60.1	0.18	-2.26	46.9	18.4	42.2	-	15
4820.339:		60.1	0.20	-1.24	-	-	-	68.0	15
4825.478		60.1	0.18	-0.86	-	-	98.3	-	15
4859.039:		60.1	0.32	-0.83	111.3	-	89.2	70.3	15
4876.112:		60.1	0.55	-1.67	-	-	34.8	30.3	15
4989.953:		60.1	0.68	-0.50	-	-	100.1	97.6	15
5200.121:		60.1	0.55	-0.49	-	-	69.4	-	15
5212.361		60.1	0.20	-0.87	95.2	102.2	75.5	66.1	15
5234.21:		60.1	0.55	-0.46	-	-	86.5	-	18
5249.576:		60.1	0.97	0.21	108.2	43.1	84.1	71.4	18
5255.506		60.1	0.20	-0.82	-	-	91.6	-	15
5276.878		60.1	0.85	-0.44	77.3	-	49.4	-	18
5287.133		60.1	0.74	-1.30	39.8	-	-	19.7	15
5293.169		60.1	0.82	-0.06	-	91.9	-	75.9	18
5311.48		60.1	0.99	-0.42	-	-	54.3	53.8	18
5319.82		60.1	0.55	-0.21	118.3	-	97.1	89.8	18
5594.416:		60.1	1.12	-0.04	-	-	118.8	73.1	17
5688.52		60.1	0.99	-0.25	-	-	58.2	53.7	17
5718.118		60.1	1.41	-0.34	-	-	29.8	33.1	17
5825.857		60.1	1.08	-0.76	-	-	30.2	-	15
6367.403	Sm I	62.0	0.18	-1.86	-	59.4	20.6	31.1	19

Table 13: Equivalent widths (continued)

Wlab	id	Z	Elow	log gf	HD 26	HD 100764	HD 198269	HD 224959	Ref
4220.66	Sm II	62.1	0.54	-1.11	-	-	46.8	38.5	20
4244.70:		62.1	0.28	-1.07	-	-	42.4	43.9	14
4318.94		62.1	0.28	-0.61	-	-	90.4	76.9	14
4424.337		62.1	0.48	-0.26	-	-	91.9	-	14
4434.318		62.1	0.37	-0.57	100.1	-	62.5	-	14
4458.509:		62.1	0.10	-1.11	-	85.1	69.7	57.8	14
4472.409:		62.1	0.18	-1.36	-	-	38.3	-	14
4499.475		62.1	0.24	-1.41	62.3	-	50.1	41.4	14
4519.63		62.1	0.54	-0.75	-	-	75.7	75.4	14
4543.943		62.1	0.33	-1.00	-	169.8	116.2	80.0	14
4566.21		62.1	0.33	-1.25	71.7	-	54.0	-	14
4577.69		62.1	0.25	-1.23	-	-	65.5	-	14
4584.83		62.1	0.43	-1.08	-	-	64.5	75.2	14
4593.54:		62.1	0.38	-1.30	-	-	52.8	-	14
4595.283		62.1	0.48	-1.02	105.3	-	77.9	44.5	14
4674.60		62.1	0.18	-1.06	-	-	85.1	-	14
4726.026		62.1	0.33	-1.84	56.4	-	33.2	40.8	14
4791.58:		62.1	0.10	-1.84	-	7.14	29.9	22.0	14
6437.64	Eu II	63.1	1.31	-0.27	-	-	-	22.2	21
# 6645.130		63.1	1.38	+0.20	hfs-syn	-	hfs-syn	hfs-syn	21
5007.234:	Er I	68.0	0.62	-0.32	156.0	-	-	101.0	14
4759.671:	Er II	68.1	0.00	-1.11	44.9	-	30.7	-	9
4820.354:		68.1	1.40	-0.48	107.6	73.9	102.5	68.0	14
4757.542:	W I	74.0	0.36	-2.43	75.2	-	36.7	-	22
4048.054:	Os I	76.0	1.90	-1.00	47.6	-	82.0	102.3	12
4793.996:		76.0	0.51	-1.99	-	34.8	18.4	-	12
4865.607:		76.0	3.79	0.31	-	70.4	65.3	-	12
4057.807	Pb I	82.0	1.32	-1.71	syn	-	syn	syn	4

1. Wiese et al. (1966), 2. Aoki et al. (2005), 3. Luck, Private communication, 4. Martin et al.(1988), 5. Fuhr et al. (1988), 6. Corliss and Bozman (1962), 7. Hannaford et al. (1982), 8. Biemont et al. (1981), 9. Wolnik and Berthel (1973), 10. Salih and Lawler (1985), 11. Andersen et al. (1975), 12. Corliss and Bozman (1962) adjusted, 13. Arnesen et al. (1977), 14. McEachran and Cohen (1971), 15. Meggers et al. (1975), 16. Lage and Whaling (1976), 17. Ward et al (1985), 18. Ward et al. (1985) (WVA), 19. Hannaford et al. (1982), 20. Saffman and Whaling (1979), 21. Biemont et al. (1982), 22. Obbarius and Kock (1982).